Towards a “fit for purpose”, fully coupled, integrated, and interdisciplinary world-Earth model - Documentation of FRIDA Version 1.0

Schoenberg, W.A., Mauritzen, C., Adakudlu, M., Blanz, B., Breier, J., Grimeland, M., Mashhadi, S., Rajah, J. K., Ramme, L. Wells, C.
Submission to the 2024 International System Dynamics Conference

Abstract

In this work we document FRIDA v1.0 a simple, box-model-type joint climate - IAM (Integrated Assessment Model) or world-Earth model. With this model we have demonstrated the importance of having a dynamically complex feedback-rich model which interconnects the climate and the human system. Representing the breadth of connections between the sectors of world-Earth system has allowed us to capture the unintuitive outcomes which arise from a more fully connected World Earth system, specifically that including climate damage in our model, reduces projections of warming. We have used FRIDA v1.0 (an admittedly developing model) to demonstrate the difficulty of reaching a 2℃ target in 2100 without relying on BECCS and other yet-to-be-tested at large-scale, negative emission energy producing technologies. The analysis based on this model shows that even in our most aggressive and unrealistically optimistic policy scenarios, we barely reached the 2℃ target on average. From the perspective of our developing modelling work with FRIDA v1.0, the 1.5℃ target is wholly unachievable without these negative emissions technologies, and more likely than not, 2.5℃ or warmer will be the result of current day levels of actions and commitment to addressing the causes of climate change.

1. Introduction: The challenges of modelling a changing world

Climate change, in all its forms, poses numerous risks and impacts to humans and ecosystems alike. When the UN Framework Convention on Climate Change (UNFCCC) was signed in 1992, these threats had already been recognized for decades (see e.g., Supran et al., 2023) - but the impacts were considered to lie far ahead in the future. However, human suffering and economic damages from climate change impacts have grown rapidly over the past 40 years (Rosvold and Buhuang, 2021). Now, the impacts are felt across societies all around the globe.

The sheer complexity of the climate change challenge has put practical constraints on global modelling communities. The division of labour between Earth system analysis of biogeophysical climate processes and integrated assessment modelling of future climate pathways for the world’s societies has caused quantitative and methodological disconnects between the various academic and user communities involved in this research. Broadly speaking, better ways to bridge across three distinct groups of researchers are needed: (1) those involved in the physical science of climate change (whose publications are assessed in IPCC’s Working Group I); (2) those researching climate change impacts, such as the vulnerability of socio-economic and natural systems to climate change, negative and positive consequences of climate change, and options for adapting to it (assessed in IPCC’s Working Group II); and (3) those involved in climate change mitigation research for reducing anthropogenic climate change (assessed in IPCC’s Working Group III). With each IPCC assessment report the collaborations among these communities have increased - but there is room and need for more integrated approaches that support investigation of the full system. Such integration is pertinent since the human World and the biophysical Earth are fully connected.

Our purpose and approach

In this paper, we document Version 1 of a fully integrated world-Earth Model called FRIDA – the “Feedback-based knowledge Repository for IntegrateD Assessments”. As the long name reflects, the philosophy of our approach is to capture current knowledge about the feedbacks within the interconnected social, biophysical and techno-economic systems, in a model which will be updated as our knowledge evolves about the dynamically changing world. Our aim is to develop and contribute a new type of model to the portfolio of Integrated Assessment Models (IAMs) that are currently used to understand the implications and feasibilities of

future climate pathways. We seek to demonstrate the value of building and using a model that captures two-way causal connections between people and planet, to use the language of the UN 2030 Agenda. We are building a model that is "fit for purpose" in the specific context of informing sustainable climate action to 2050, in line with the goals of the Paris Agreement and the priorities of the European Green Deal. And an important priority for us, given our intention to bridge across academic and user communities, is to build a model that is transparent to contributory experts and users alike.

Informed climate policy discussions should take into account delays, feedbacks and the complicated interlinkages within and between the physical climate and human activities. However, coupling detailed process-based IAMs to even more detailed ESMs would result in models that are both extremely computationally intensive and potentially completely opaque. Instead, our approach to building FRIDA has been to focus on important biophysical and social system feedbacks. This entails keeping disaggregation to the minimum level that supports a reasonable representation of each subsystem. The model is global, representing variables of universal importance, such as average wellbeing and health, atmospheric and oceanic temperatures, aggregate emissions and so forth. There are several advantages of this clarity-before-detail approach. Computational simplicity gives us the ability to quickly run and thoroughly understand "what-if" scenarios. It also allows us to explore the uncertainty domains by quickly running thousands of simulations. Due to the lower complexity of the model and its clear diagrammatic representation, the model and the analysis methods are transparent, both to subject experts working with the model and the eventual end-users of its analyses and insights.

An essential part of being fit for purpose is that FRIDA, as a knowledge repository, must be suitable for its intended users and use-contexts. To that end, we have prioritised three user groups whose respective needs determine the way in which the model is designed and deployed.

Our first target user is the **global change expert**, say, a typical IPCC contributor, who is frustrated that the climate challenge, which in reality is fully interconnected and requires interdisciplinary understanding, gets addressed, taught and studied within disciplinary silos. Our second target user is the **decision-maker** who would normally use IAM-based analysis to inform their decisions about climate action, and who may be confused about the lack of transparency in existing pathways and analyses of policy options. Our third target user is the **engaged citizen** who is concerned about the climate challenge, but lacks the knowledge needed to engage in and catalyse a deeper societal discussion on the topic.

FRIDA is built to be fit for all these use-contexts, although the interface tools for using and learning from FRIDA take different forms for the different user types. For instance, scientists in the global change research community may wish to "dive under the hood" of the model and investigate its actual couplings and parameter settings. Decision makers may prefer to use an interactive learning tool to get quick answers to "what if" questions. And engaged citizens may only wish to interact with a very simplified version of the model – for instance, through an interactive dialogue or game experience based on the model. By continually engaging with potential users, iteratively developing the model with low-complexity and transparent features, and by holding the model construction to the highest scientific standards, our aim is that FRIDA will be a world-Earth model that is transparent, fit for purpose and widely used in these user communities.

Overview of paper

We present, in Section 2, a brief overview of our modelling method of choice, System Dynamics, and an overview of existing world-Earth models developed within that framework. We further detail our step-by-step approach to our modelling process. In section 3, we provide the documentation of FRIDA v1.0, both an overview of the model structure and the more detailed (module by module) description. Section 4 describes the calibration and behaviour validation process employed for FRIDA and its results. In Section 5, we present what we call our "Current Policy Analogy" scenario, which in reality is our baseline scenario. In this scenario we have used one external policy lever - namely investments in various types of energy - to establish a scenario that is comparable

to the 21st century temperature projections that result as a consequence of current policies reported to the UNFCCC in accordance with the Paris Climate Agreement (Climate Action Tracker, 2023). Then, in section 6, and 7 we proceed to introduce two sets of policy scenarios that build upon one another striving to reach a 2 degree Celsius warming target in 2100. We evaluate these results both with and without climate feedbacks to the human side of the system. Finally, in section 8 we lay out the next steps in the development of FRIDA v2.0.

2. Methods

Modelling method: System Dynamics

System Dynamics is a computational modelling methodology based on systems of differential and difference equations (see e.g., Forrester 1961, Sterman 2000, Ford 2010). Central to the method is the feedback perspective, which privileges the representation of complex and oftentime circular interactions between system components that endogenously generate behaviour. Such complexity is often presented in stylized stock-and-flow diagrams. This allows for clarity when representing and analysing complex feedback systems. Since many climate-related models are also based on differential equations this allows inclusion of these models directly with only a modest adjustment of notation. This has the advantage of grounding our work in well-established science, speeding our model development, and also simplifying inspection of FRIDA by others working in the various disciplines we draw on. We use Stella (isee systems, 2023) as our common modelling platform, which allows the parallel development of different modules while retaining the ability to continuously work with the integrated model. Stella also makes it easy to work with, and integrate, time series data measurements such as GDP into modelling which is used as part of the calibration process described in Section 4.

The System Dynamics landscape of integrated global models

Modelling global change issues within the system dynamics framework is a road well-travelled. Here, we briefly describe the three most well-known System Dynamics global system models that come before FRIDA: WORLD3, En-ROADS/C-ROADS and FeliX.

WORLD3: The WORLD3 model was the basis for the 1972 “Limits to Growth” book (Meadows et. al 1972, 1974). Commissioned by the Club of Rome, the work was built upon the book “World Dynamics” (Forrester, 1971). The simulation model studied the interactions between four global scope subsystems: population, industry, pollution, and nonrenewable resources, tying them all together with an endogenous model of global development. Over time the model has undergone further development and application, featuring in books such as Beyond the Limits (Meadows et al. 1993) and Limits to Growth: the 30 year update (Meadows et al. 2004).

En-ROADS & C-ROADS: En-ROADS (Energy Rapid Overview and Decision Support) (Siegel et al., 2018) is a simulation model developed by “Climate Interactive” that allows policy makers and the general public alike to test different policies for addressing climate change. The model simulates interactions between energy production, consumption, land use, transportation, industry and climate change. The model provides a simple to use intuitive web-based interface, which gives end-users a plethora of policy options and assumptions to explore in their quest to reduce global temperature increase in the year 2100. En-ROADS was based on C-ROADS (Siegel et al, last updated Aug 2023), which is used to model the carbon cycle for assessing greenhouse gas emission reduction policies. Documentation of EN-ROADS and C-ROADS can be found online here: https://docs.climateinteractive.org/projects/.

FeliX: FeliX (Full of Economic-Environment Linkages and Integration dX/dt; Eker et al., 2019; Rydzak et al., 2013; Walsh et al., 2017)) was built to assess the economic, social and environmental benefits of earth observations. It aims to represent a strongly interlinked Earth system and socio-economic system components, forming a complex dynamic system. It consists of nine sectors, namely Economy, Energy, Emissions, Carbon Cycle, Climate & Environment, Population, Technology, Land Use, Energy and the Global Earth Observation System of Systems (GEOSS). All model sectors are highly interrelated and bring the global perspective to the GEO benefits assessment. In order to bring some of the GEO benefits assessment public, a simulator based on

the FeliX model was developed, equipped with a user-friendly interface. The first version of the model was developed by Felicjan Rydzak and Michael Obersteiner. Between 2014 and 2017, FeliX model maintenance and development has been led by Brian Walsh. Currently, the model maintenance and development is undertaken by Sibel Eker. Documentation can be found here: https://druptest.iiasa.ac.at/staff/sibel-eker

The step-by-step approach to building FRIDA

FRIDA v1.0 builds upon the pre-existing work in the System Dynamics field, aiming to represent as much dynamic complexity as possible (like WORLD3) while simultaneously striving to include only the most important aspects of detail complexity. As a consequence of our desire to represent the combined world-Earth system in a process oriented, and rigorously calibrateable way FRIDA necessarily has to include more detail complexity then WORLD3. FRIDA also attempts to avoid emphasising the internal dynamics of any one sector of the combined world-Earth system above another (unlike En-ROADS, which focuses on energy systems), instead choosing to focus as much as possible on intersectoral connections (as FeliX does, but with a higher level of aggregation).

The System Dynamics modelling process starts with defining the problem behaviour intended to be explained by the model. In the case of FRIDA, the fundamental behaviour is **Surface Temperature Anomaly (STA)** – the temperature of the air at the surface of the Earth, which is a good proxy for the kind of climate humans live in. Projections for temperature change in the present century vary by about the same amount, depending on future scenarios for changes in greenhouse gas emissions, the response of the climate system, demography, economy and so forth. **STA is the fundamental variable in FRIDA,** in System Dynamics language: the variable whose behaviour we seek to explain.

Where possible, when building FRIDA we made use of pre-existing models in the literature making only the smallest changes necessary for them to meet our purposes. Three such examples of this are our use of FaIR (Leach et al. 2021) as the basis for our temperature calculations, our use of components from BRICK (Wong et al., 2017) and MAGICC6 (Nauels et al., 2017) as the basis for our Sea Level calculations, and the use of MIND (Edenhofer et al. 2005 and Held et al. 2009) as the basis for the Energy calculations. In the cases where there were no readily available models that were fit for purpose, we applied the standard system dynamics method as documented by Forrester (1994): To explain changes in the fundamental variable, which often tends to be a stock (a variable that accumulates or depletes over time), one identifies all the flows that influence that variable, making it change. In the case of STA, the flows involve greenhouse gas and aerosol emissions that make the concentration of carbon dioxide and other greenhouse gases in the atmosphere change, and flows of greenhouse gases that deposit into land and ocean. Working backwards, those flows originate from other variables that need to be identified (and in turn, the preceding variables of those need to be identified).

The next step is to run the model to see how the variables change over time for a period during which time-series data are available (here, 1980-2020). If the behaviour of the variables do not compare with observations, it is either because key processes and feedbacks are missing in the model, or because the initial conditions for the variables, or the parameters which control the relationships between them, are poorly chosen.

The calibration-validation process

So the third step is to use the observed time-series for as many variables as possible and compute which initial values and parameters values would create the smallest root-mean-square error between observations and variables, collectively. This is the calibration phase.

Then, iteratively, one expands the stocks and flows, including more processes and more feedbacks, and reiterates the calibration phase until the behaviour of the stocks matches observations, within limits set *a priori*. At this point one is satisfied that the model is structurally and behaviorally valid. During this phase, it is important that the expansion is based on documented knowledge (whether it comes from the laws of nature, empirical relationships or expert opinion). This is the validation phase.

Making the model fit-for-purpose

The next phase involves making the model fit for purpose. If the purpose of the model is to identify for citizens ways in which they can contribute to minimising climate change, for instance through dietary shifts or driving habits, then the model needs to include stocks and flows that relate to those shifts (for instance: greenhouse gas emissions from road traffic) so that they can evaluate why and how that would help. If the purpose of the model is to support decision makers responsible for suggesting new policy instruments for mitigating climate change, then it is important that the model includes emissions from all the main sectors (industry, agriculture, waste management, energy production etc.) so that they can compare and decide upon what they think is most efficient.

Scientific analysis

The next step is to analyse the structure of the model – to find out what are the main feedbacks, the main delays, the most sensitive parts of the system, the most likely parts for regime shifts and so forth. In short, to explain how the system works to produce the identified behaviour of interest. This part is particularly important for research, and is more attainable with simpler models.

Future projections

And finally, the model can be used to run future scenarios. The base scenario is often chosen as the one in which one assumes that all the relationships from the observed period (1980-2020) remain the same in the future. But the base scenario can also be tuned to describe a particularly interesting case (as we have done in this paper, see section 5). All other scenarios are compared to this baseline. Often, the other cases are related to policy changes, such as changing the carbon tax. But it can also relate to changing a relationship on the climate side, for instance testing the importance of the melting rate of ice sheets.

During all these steps, it is essential to include uncertainty estimates because, during the model calibration phase, there are multiple possible combinations of parameters which can, and oftentimes do produce acceptable behaviour. Our uncertainty estimation measures the uncertainty in the calibration process, and generally follows the approach described by Wakeland and Homer (2022). A global sensitivity analysis (Saltelli 2008) is run using Sobol Sequence sampling across all the relevant calibration parameters (and their associated ranges) in the model. We then specify a threshold value for the RMSE (root mean square error) of the model vs. the calibration data as a cutoff to determine which runs are acceptably calibrated in history, and therefore are kept in the resulting uncertainty dataset. The range in future projections caused by the differences in initial conditions and parameters values under one combination of policies is the parametric uncertainty inherent in the model.

Other sources of uncertainty, associated with, for example the definition of the system boundary and structural uncertainties in the model itself, i.e. the way we chose to represent real world relationships, are much harder to quantify in the simulation results. There are also uncertainties in the observed behaviour data that we use to calibrate the model to, and the potential for errors in model construction and output data processing (Kwakkel et. al, 2010). During the development of the model we strive to make as few constraining assumptions as possible to allow the parametric uncertainty to describe as much of the overall uncertainty as possible. Where that isn't possible we document the logic and the reasons for the constraining decisions that we have made, and where possible discuss the impact of those assumptions on results.

3. FRIDA v1.0

FRIDA is organised as a series of interconnected modules - the root level of which is depicted below (Figure 1).

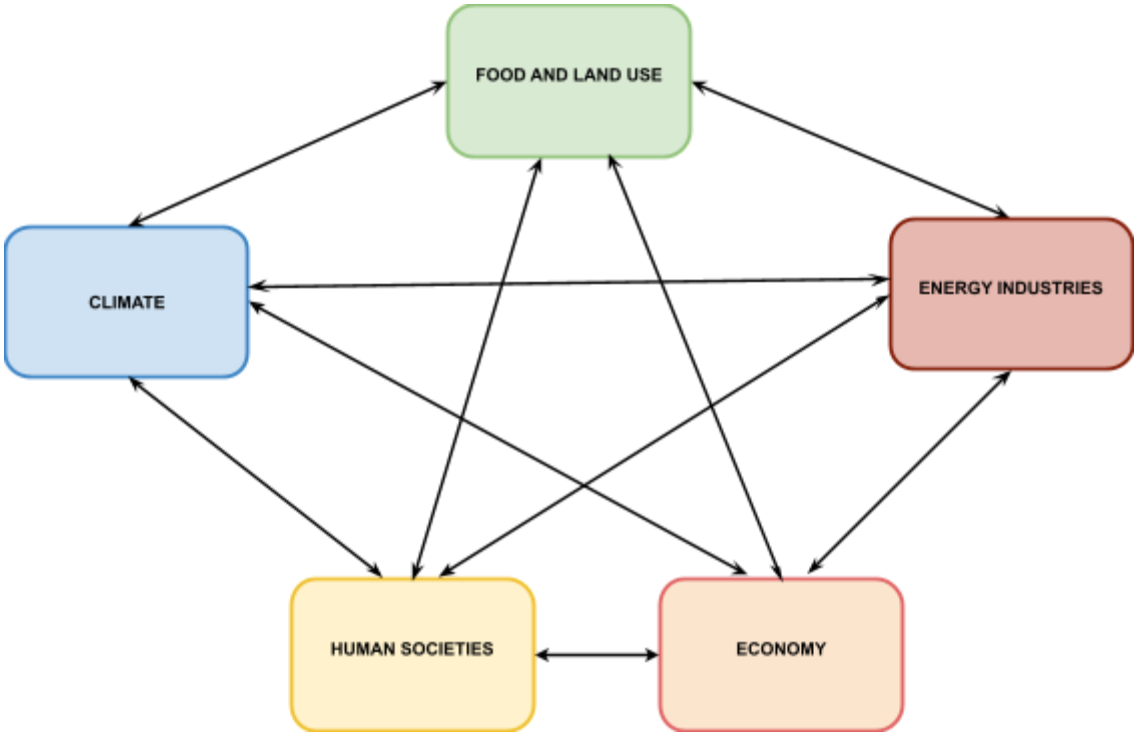

Figure 1: The FRIDA modules, showing the strong emphasis on connectedness and feedbacks.

All these modules have their own specific role in the sequence of events that take place in the world-Earth system when it is disturbed by human activities: The “Energy Industries” extract fossil fuels, refine them (for instance in terms of liquid fuels for use in cars and trucks) and generate electricity (often from coal). Within the “Food and Land Use” module the agriculture industries generate crops and livestock for food production. Also, all activities that generate changes in land use (such as cutting of forests) are accounted for in this module. Both modules result in emissions of warming greenhouse gases and cooling aerosols.

The demand for all of these activities come from the “Human Societies” module, closely aided by the “Economy” module. And all end up in the “Climate” module, where concentration of greenhouse gases and aerosols in the atmosphere determine the changes in STA and sea level. In turn, climate change impacts the other modules, for instance, heat waves can cause premature death, droughts can cause crop failures and forest fires. We model the “climate damages” as a function of STA. The impacts are normally very costly, they affect our industries, our economies, our food supplies, in short: the way we live.

In FRIDA, information is carried both ways, from humans to nature, and from nature to humans, including all the self-reinforcing mechanisms that exist in such a complex system. The only real levers exist in the “Human societies” module, where action can be taken on personal to political levels. In our effort to make FRIDA “fit for purpose”, we work out with our identified users what levers would be particularly interesting, and what measures we should use to compare the various levers against each other.

The main variables and flows of FRIDA v1.0 are depicted in Figure 2. As mentioned, the behaviour we attempt to explain (the “fundamental variable”) is STA. The radiative imbalance that occurs as a consequence of man-made emissions (of greenhouse gases and so forth) first and foremost changes the temperature. As a consequence, a slew of other changes take place, such as sea level rise, precipitation changes, ice melt, ocean acidification, extreme weather - the list is lengthy, and the impacts are usually damaging to society. In FRIDA v1.0, we only include a limited set of these consequences and use for instance temperature as a proxy to define “climate damages”, climate impacts that damage the other modules in one way or the other.

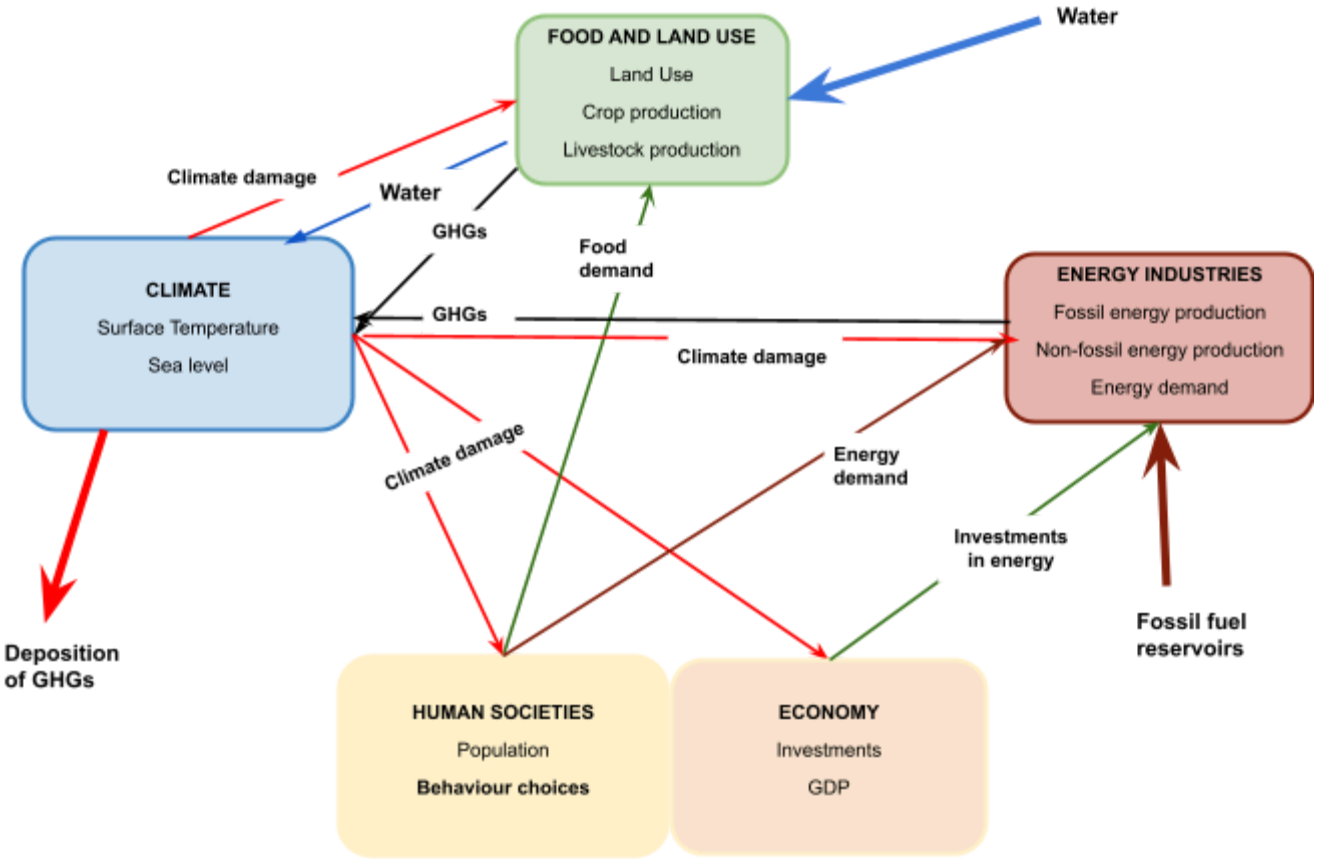

Figure 2: The modules, interactions and main variables of FRIDA V1.0. Red arrows are climate damages. Blue arrows are water impacts. Green arrows are human impacts. Brown arrows are energy flows. Black arrows are greenhouse gas emissions.

The cycle of carbon starts with the fossil fuel reservoirs in the ground (on the lower right hand side in Figure 2. These are extracted depending on the energy investment strategies in the model (this is the one external lever we use to set the baseline scenario in section 5). Greenhouse gases are emitted from the energy industries module (from extraction and production of energy) and from the food and land use module (cutting of forests, raising of livestock and so forth). All these emissions contribute to the rise of GHGs in the atmosphere, which results in rising temperature. Not all the GHGs end up in the atmosphere, however, some is stored in the ground (in land and ocean). This process denotes the end of the carbon cycle, on the left side in Figure 2.

The STA (calculated in the climate module) and all its climate consequences are cycled back into all the other modules as "climate damages", creating changes and feedbacks within and between each module. The six climate damages that are implemented in FRIDA v1.0 impact: 1) mortality rate, 2) energy capital, 3) energy demand, 4) crop yield, 5) water lost to evapotranspiration, and 6) failure rate of loans.

We will describe each module in greater detail below, but keep in mind that we use data from the period 1980 to 2020 to calibrate the interrelationships between variables (using the method described in the step-by-step approach from the preceding section).

Description of subsystems

Human societies module

Given that it is people that cause anthropogenic climate change, it seems natural to begin with the "human societies module". In future versions, we intend to incorporate behavioural choices that are relevant for the climate change problematique, such as dietary and transportational choices, but in the current version the key structure is the demography of the population (age distribution, births, deaths and so forth).

Population

Population is modelled as a "continuous cohorting system" (Eberlein and Thompson, 2013), using Stella's (isee systems, 2023) conveyors, to represent the dynamics of ageing along with age-group specific mortality. The continuous cohorts are grouped into 6 age categories: Infants, Aged 1-20, Aged 20-40, Aged 40-60, Aged 60-80, Aged Over 80 for the purposes of simulating different mortality rates. These age groups were chosen based on their distinct age specific mortality rates. The age-specific cohorts are initialised using United Nations (2022) data of global population by age in 1980.

The age-group-specific mortality rates are calculated based on regressions using GDP per person as the input (from the Economy module), because increasing GDP per person places downward pressure on death rates (Miladinov, 2020). The other factor used to determine respective death rates is climate damage; specifically a calibrated reinforcing impact of the STA (from the Climate module) on each death rate, capturing the demographic impacts of sea level rise, mass migration, etc. (IPCC, 2022). Births are based on a calculated fertility rate, the result of a calibrated regression using GDP per person as an input, the rationale being that with rising standards of living and education, birth rates drop exponentially (Kirk, 1996; Lesthaeghe, 2010; Marquez-Ramos and Mourelle, 2019, Proto and Rustichini, 2013).

Economy module

The Economy Module is depicted in Figure 3. The economy is sensitive to climate damages through changes in the default rate of loans. The most direct impact of the economy in terms of sustaining or mitigating climate change is realised through investments in energy. We have implemented a Schumpeterian model of economic growth, including rudimentary monetary and financial dynamics. It features a circular flow that grows in a cyclical pattern due to finance-mediated investment. The module emphasises finance-mediated credit provision as a central driver of growth (King and Levine, 1993).

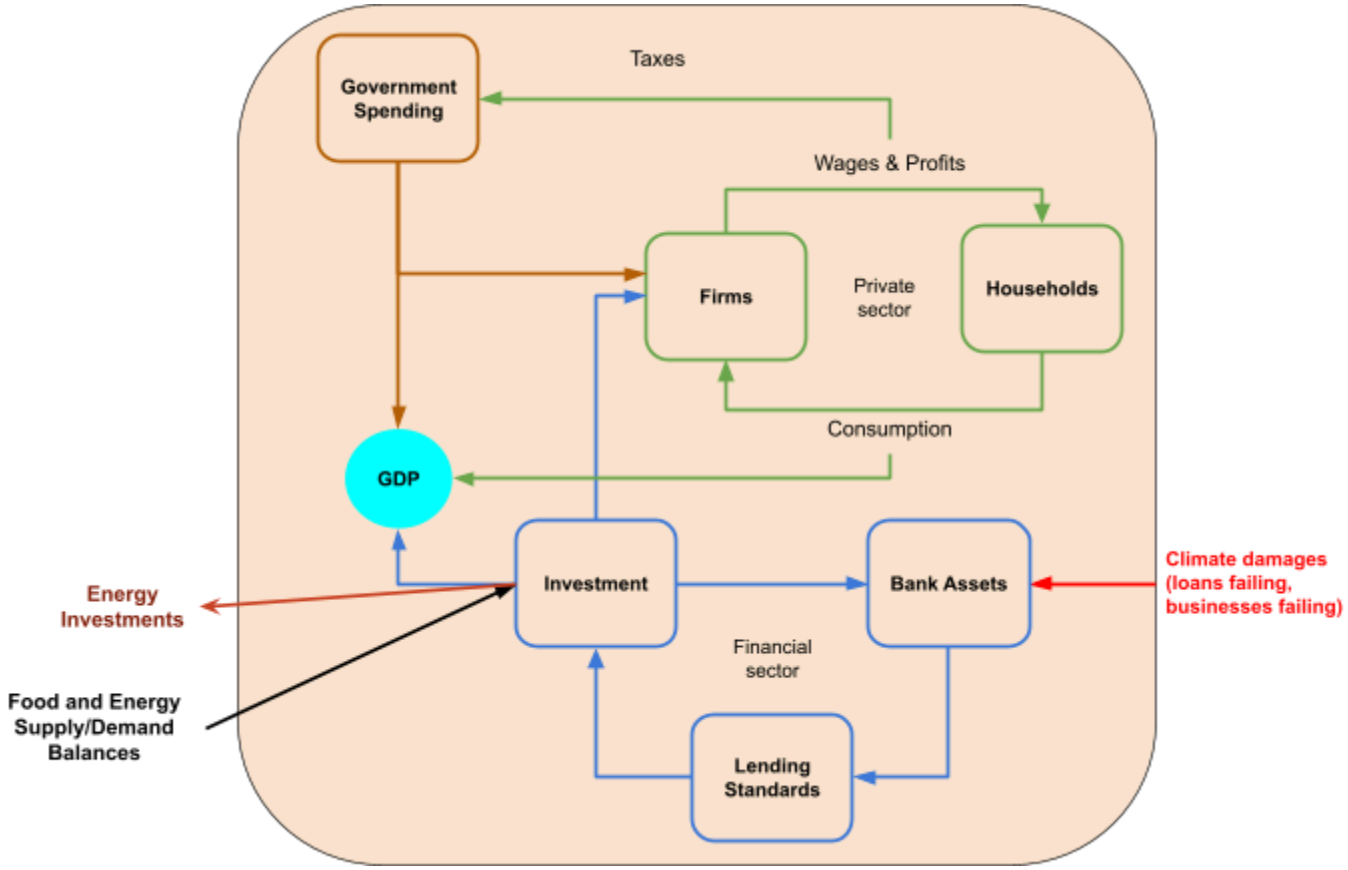

Figure 3: the Economy module in FRIDA v1.0. Green represents the elements which generate the consumption part of GDP. In blue

are the investment parts of GDP, and in brown, the government parts of GDP. The "private sector" forms the basis of government spending through taxation. The "financial sector" generates investments via lending standards, and the banks desire for profits.

The module calculates global GDP as the sum of the purchase price for final uses of all goods and services. Functionally, it is the sum of total investment, private consumption, and government spending added together. The three components of global GDP are each endogenously generated by their own subsector of the economy module: investments by the financial sector; private consumption by the production sector; and government spending by the government sector. The module is stock-flow consistent: money is endogenously created and all monetary flows and stocks are consistently accounted for (Nikiforos and Zezza, 2018).

Investments

Investments are funded by credit, and credit expansion generates economic growth. Credit expansion is driven by savings accumulation and the financial sector's profit incentive. The true quality of the loans generated is unknown *ex ante*: "bad" loans are discovered when the borrowers default. Whether a loan is good or bad depends on the lending standards of the bank during origination, which are reactive to profit incentives and the present default rate (Dell'Ariccia and Marquez, 2006). There is also a marginal effect of temperature, as global warming will degrade the natural environment's ability to support investments. The ratio of bad loans indicates financial fragility.

This banking structure allows a more fragile representation of the economy than the typical Solovian approach based on an aggregate production function. Growth and economic stability increase the banks' tolerance for risk, putting upward pressure on the banks' lending volumes, and downward pressure on their lending standards (Asea and Blomberg, 1998). Credit expansion produces yet more growth, but also fragility, that can eventually lead to crisis and recession (Loayza and Ranciere, 2006). These mechanisms conspire to produce business cycles which interplay with the other modules of the FRIDA model.

The choice of how to distribute investments in energy between the different production technologies is (in this version of FRIDA) left to the user. The user is offered three premade scenarios fossil focused, balanced, and emissions reductions focused, but can also design another scenario. The total amount of energy investments is determined endogenously with the aim of balancing energy supply and demand.

Private Consumption

Private consumption is modelled in the interplay between households and firms. Households are disaggregated into workers and owners, who are paid wages and profits, respectively, by the firms, including financial firms. The owners and workers in turn consume a fraction of their income, generating revenue for the firms. The remaining income is saved, according to a saving target set as a multiple of their present income. The sum of owner, and worker consumption is the private consumption component of GDP. Consumption and savings grow with economic growth.

Government Spending

The government sector produces government spending as its output, based on income raised through taxes on wages and profits. The amount of spending is a function of the ratio between government debt and GDP, a rough indicator of fiscal health. The difference between government spending and income accumulates as government debt, a component of the banks' assets. Government spending increases the firms' income, and therefore both wages and profits, compensating the dampening effect of taxation.

Energy industries module

Energy production and combustion has been responsible for the vast majority of anthropogenic greenhouse gas emissions for the past hundred years. The **Energy Industries module** is depicted in Figure 4. The primary relationship is that between production and demand of energy (the energy balance). This module produces

greenhouse gases, primarily CO2. Climate change affects both energy production (through infrastructure damages) and energy demand (need for cooling and so forth).

Figure 4: The energy industry module in FRIDA contains stocks for fossil and non-fossil energy production technologies with feedback to the economy and climate modules. The red arrows represent climate damage in the form of infrastructure damage. The green arrows indicate flows of money (investment) into the construction of capital. The supply demand balance is the ratio of energy supplied, to energy demanded, and that balance (implicity representing price) impacts investment in the economy.

The energy system modelled in FRIDA is based on the Model of INvestment and technological Development (MIND) presented in Edenhofer et al. (2005) and Held et al. (2009). The MIND model was developed to optimise the energy transition and answer the question of how to achieve the cheapest transition that keeps emissions low enough for the temperature to not cross a temperature guardrail, such as the two degree target. In MIND, energy is provided by different sources which are driven by investments. The energy sources include fossil energy, renewables and traditional non-fossil energy. Fossil energy is produced in two steps: resource extraction and energy generation. The productivity of resource extraction depends on the limited resource base and extraction knowledge. Secondary fossil energy production depends on extracted resources and fossil energy generation capital. Renewables are modelled with a vintage structure and "learning by doing". Learning by doing means that as more is invested into renewable energy or resource extraction, installation costs go down. The motivation is that research into renewable energy, which can reduce costs, is mainly driven by economic activity surrounding the expansion of renewable energy. Other traditional non-fossil energy is included as an exogenous time series. Energy is aggregated and consists of both electricity and all other forms of energy.

The energy module in FRIDA (Figure 4) has four major differences to that in MIND: disaggregation of the various energy sources, several energy investment user choices, explicitly modelled energy demand and, finally, the energy industries can be impacted by climate damages. We will discuss these in the following.

Fossil Energy Production

Fossil fuel **extraction** depends on the available stock of extraction capital. Investments into fossil fuel extraction decrease the cost of installing further fossil fuel extraction capital because as the knowledge needed for fossil fuel extraction (location of deposits, extraction technology, etc.) increases, the cost of extraction decreases (the "learning by doing" effect). However, scarcity of available fossil fuel stocks decreases the effectiveness of the fossil fuel extraction capital. Fossil energy **production** has two inputs: Fossil fuels and fossil energy capital. These inputs are weak substitutes for each other, allowing for a more capital intensive production process requiring less fuel and vice versa.

Non-fossil fuel energy production

Non fossil energy production is split up into solar and wind energy, hydropower, nuclear power, and other energy. Each of these is modelled explicitly. This is done in order to have a better match with real installation cost curves. Installation cost curves differ significantly between the different non-fossil energy technologies. While solar PV and onshore wind have seen very rapid cost reductions in recent decades (Budischak et al. 2013), the average installation cost for hydropower across the globe presented an overall increasing tendency (Forouzbakhsh et al. 2007), reflecting the limited locations where hydropower can easily be installed, requiring the installation in more challenging areas at greater expense. Solar and wind energy production follows the vintage capital structure found in the MIND model. This allows for learning by doing effects to increase the effectiveness of newly installed capacity without simultaneously increasing the effectiveness of old installations. The installation costs of hydropower depend on the amount of installed capacity. It is assumed that locations where hydropower can cheaply be installed are utilised first, with increasing costs for subsequent installations. The installation costs for nuclear power plants follow an exogenous time series based on the historical trajectory of installation costs (Schlissel and Biewald, 2008). Installation costs of other energy provision are assumed to be decreasing with time, limited by a fixed floor cost.

Energy demand

The energy module in FRIDA contains a model of energy demand driven by GDP and overall investments (from the economy module of FRIDA), the STA (from the climate module of FRIDA), and population (from the human societies society module of FRIDA). The per person use of energy depends on the logarithm of the GDP per person. The STA increases the per person energy demand linearly. Total energy demand is calculated by multiplying the per person energy demand with population. The per person use of energy can be further influenced through a policy lever (see table 3) in this version of FRIDA.

Climate damages: Stocks of energy production capital, as well as the demand for energy, can be impacted by climate induced damages. These are related to the global surface temperature anomaly calculated in the climate module of FRIDA.

Energy imbalance impact on the economy

The energy supply balance is calculated as the fraction of **production** over **demand** (physically, of course, it is the difference between the energy production and the energy demand). The relative supply of energy impacts the economy via an implicit price mechanism. For instance, when the supply does not meet demand, it decreases investments within the economy module (as high energy prices would make investments less likely to succeed) which can cause a recession (figure 4).

Food and land use module

Agriculture and land use change explains most of the rest of the anthropogenic greenhouse gas emissions (when energy-related emissions are accounted for). The Food and Land Use module, depicted by Figure 5, simulates the land use of habitable land driven by the population. It is mainly subdivided in forest land, grassland and cropland. Land reallocation is one of the major cycles in this module, and any net change in land use will result

in greenhouse gas emissions (positive or negative). Both livestock and crop production impact the amount of available food as well as the net emissions of greenhouse gases (CO2, CH4, N2O) and SO2. Climate change affects crop yield, water lost to evapotranspiration and soil carbon emissions.

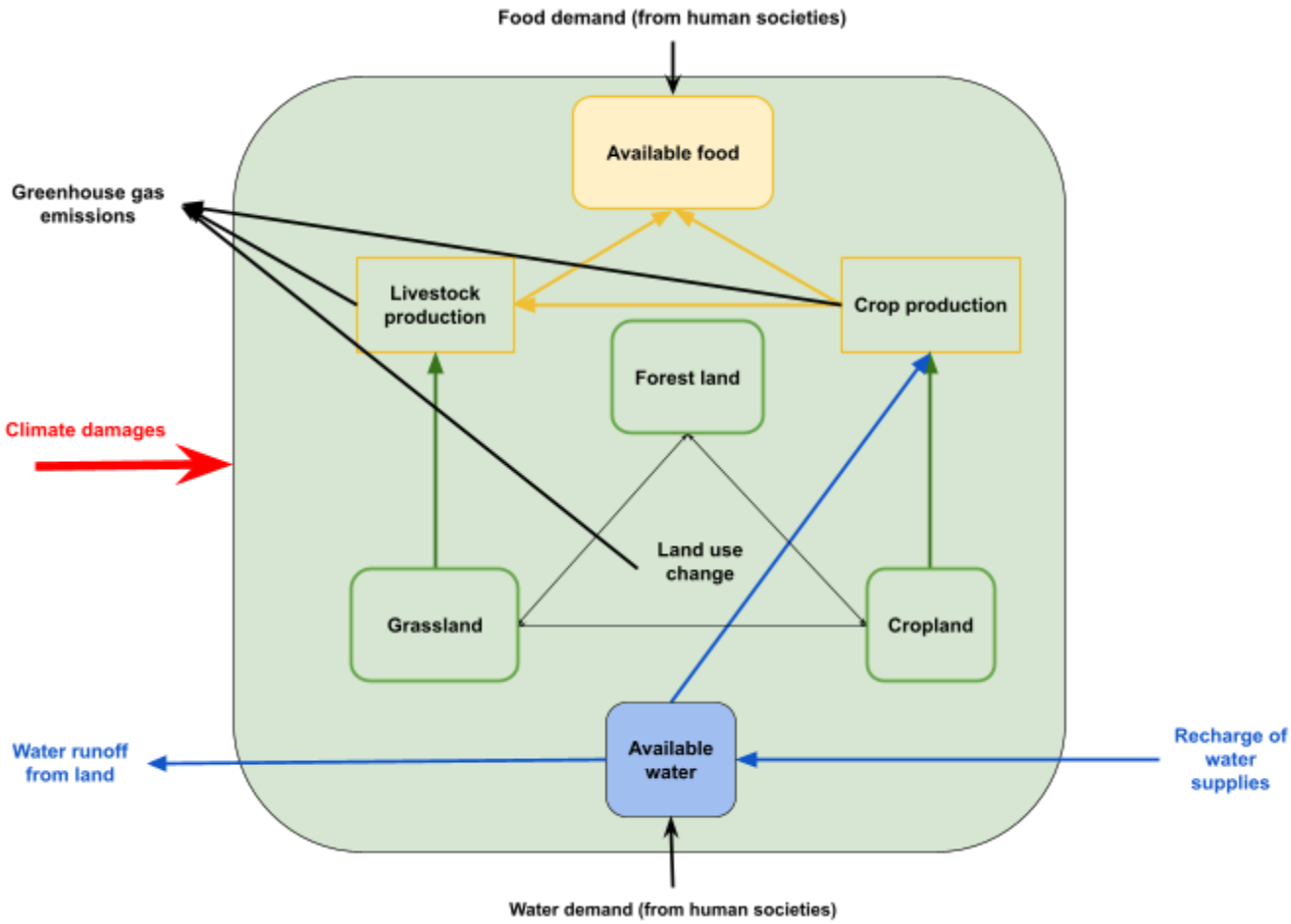

Figure 5: The Food and land use module includes a representation of habitable land (green borders), separated in different land stocks. Food production (yellow) is divided in livestock and crop production. The module has a functional representation of water availability (blue) to simulate water limitation. The population and the climate module have a direct effect on livestock and crop production.

Land Use

Depending on the demand of livestock and crops as well as the productivity of land, grassland and cropland can be converted by processes such as ploughing up grassland and deforestation for an increase in crop production or by fallowing cropland or deforestation for an increase in livestock production. Afforestation that converts grassland into forest land is implemented as a policy instrument that can be applied. Reforestation describes the process of converting deforested forest land used as cropland back to forest land. Both arable land and grassland can be degraded by overuse. This applies in particular to dry regions and those with vulnerable ecosystems.

Crop and livestock production

Livestock production is either based on rangeland (grassland) as a food source or a ratio of crop production. Crop production is a product of cropland and crop yield. Crop yield is a function of crop demand, fertilisation, irrigation, soil quality and the climate response. Demand for crop as well as livestock production is calculated on the basis of population times per capita demand, which is a function of GDP per capita. An increase in livestock production also increases the demand of crop production as more crops have to be produced as feedstock for livestock. Fertilisation consists of man made fertiliser and manure application which is driven by fertiliser use as well as livestock production. Soil carbon in cropland is used as a proxy for soil quality (Lal et al. 2015) and is implemented as an additional stock which has crop residues, a byproduct of crop yield, as input and CO2 emissions as output. Increasing soil carbon has a positive effect on crop yield (Lal et al. 2006). Irrigation is

limited by the available water supply, a balance equation between the natural recharge rate and and the total withdrawals including agricultural (irrigation) and non-agricultural withdrawals.

Greenhouse gas emissions

Fertilisation that consists of man made fertiliser and manure application are a main source for N2O emissions. Additionally livestock production is the main source for CH4 in the system. CO2 has different sources. The decomposition of soil carbon leads to CO2 emissions, whereby the net effect in offsetting against the inputs (crop residue amount) determines the actual quantity. Together with deforestation (and afforestation as a negative effect), they form the current calculated CO2 emissions from the module.

Climate damages

The impact of climate change on the food and land use module is two-fold: CO2 fertilisation, which has a positive effect on crop growth, and the STA, which has a negative effect globally. The net effect is negative, as CO2 fertilisation is less effective (Long S.P. et al. 2006).

Climate module

The climate module (Figure 6) incorporates the entire biogeochemical system that we call Earth, or nature, with the exception of some aspects of land and water use. The main variable of this module (as of the entire model) is **STA**. Two other variables, **atmospheric concentration of greenhouse gases** and **sea level** are of key importance, the former to calculate the temperature and the latter to broaden the scope of climate damage calculations in the model. The module receives greenhouse gas emissions from the other modules and returns information about climate change to the other modules.

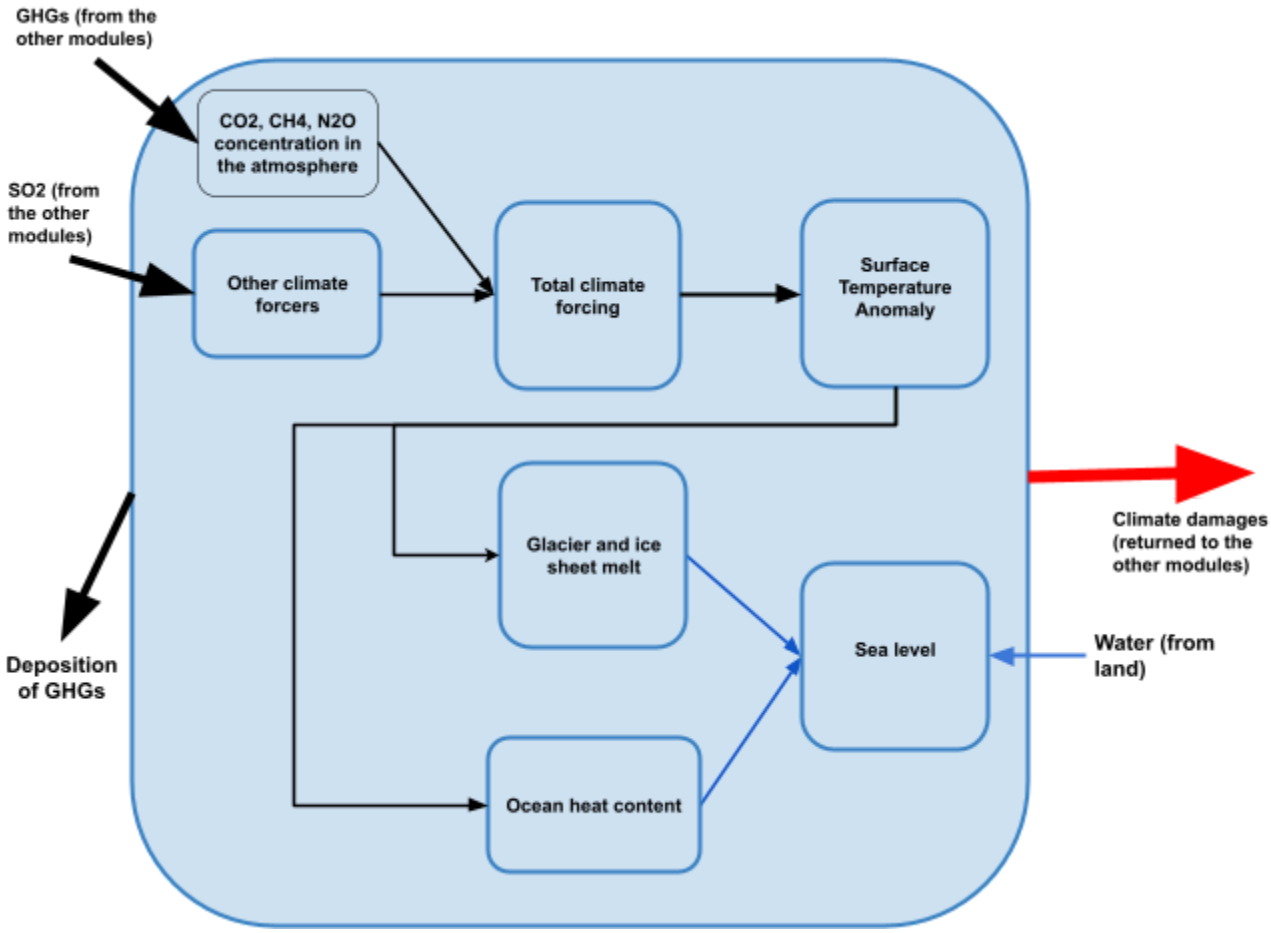

Figure 6: the Climate module. Emissions from other modules are input, with the climate forcing of these four species calculated. Other forcings are then approximated from these emissions (Ozone, CFCs & F-Gases, and the effect of black carbon on snow; see text), with volcanic and solar forcings input externally. The resultant total climate forcing is then applied to an energy balance model to calculate the temperature response. This is used to calculate climate temperature-related damages and sea level rise.

Emissions of the three most important greenhouse gases are interactively tracked: CO2, CH4, N2O, as well as SO2 (which produces (cooling) aerosols). CO2, CH4, and N2O emissions originate from all three modules; SO2 from the Energy Industries and Food and Land Use modules only (though in the Food and Land Use module SO2 emissions are assumed to be a constant 2.1 MtSO2, based on the historical average values of emissions from biomass burning sources over the past 40 years (Marle et al. 2017)).

From greenhouse gas emissions to temperature using FaIR

To calculate surface temperature anomaly, we use the FaIR Simple Climate Model (Smith et al. 2018; Leach et al. 2021) as a starting point. FaIR takes exogenous inputs of 64 relevant species (greenhouse gases, aerosols, and other climate forcers) and calculates concentrations of GHGs, radiative forcings, and STA. In the philosophy of the FRIDA model (to be as simple as possible), we calculate explicitly emissions of only the most important species, namely CO2, CH4, N2O, and SO2. These species are represented in FRIDA in the same way as in FaIR.

In FRIDA, atmospheric concentrations of CO2, CH4, and N2O are tracked as stocks and calculated as in FaIR. Flows of emissions enter at each timestep, with removals calculated in accordance to their atmospheric lifetimes. These lifetimes are modified by different climate variables, accounting for feedbacks within the system. CO2 is tracked in four separate stocks, with four different baseline lifetimes, which are in turn modified by CO2 concentrations, cumulative CO2 emissions, and STA. N2O and CH4 are tracked as a single stock each, with CH4's lifetime affected by CH4 concentrations and STA, and N2O's by N2O concentrations.

From these concentrations, the radiative forcings due to each of these species are calculated. Aerosol forcing is calculated from SO2 emissions rather than concentrations, since SO2 is a short-lived species. Then, three remaining types of forcing were modelled as functions of the actively modelled forcings: Ozone, CFCs & F-gases, and black carbon (BC). Historical correlations between the emissions of one or more species modelled in FRIDA and the target forcings were found and used to derive the most appropriate relationships. The suitability of these fits were further tested using future projected forcings in the IPCC AR6 scenario database, and they are shown in Figure 7. Specifically:

- Forcing from Ozone was modelled as a multi-linear function of SO2 and CH4 emissions. Ozone is produced chemically from reactions of short-lived forcers, and is short-lived itself, so this mix of precursors are plausible appropriate correlators for Ozone production. This approximation reproduces historical and plausible future Ozone forcings well.

- Forcing from CFCs & F-gases was modelled as a linear function of N2O emissions. The link between these forcings is less clear, as these species originate from different sources on different timescales; this correlation presumably arises from the fact that emissions of all species has generally increased historically, though the time series for CFCs and F-gases begins to ramp up substantially later (around the 1950s) than most other species. This relationship is therefore substantially less accurate than that for Ozone, with errors around +-0.1W/m2 at different points historically. The effect of CFCs and F-gases is therefore a potential candidate for future explicit simulation within FRIDA.

- Finally, since black carbon (BC) is not simulated within FRIDA, the forcing attributed to its effect on Earth's albedo via darkening ice regions is modelled as a multi-linear function of SO2 and CO2 from land use. A correlation with SO2 is plausible since both are short-lived combustion by-products, with the link to land use CO2 less directly clear given their different lifetimes, but not unsuitable given their sources. This relationship is reasonably accurate, and is in any case a small forcing.

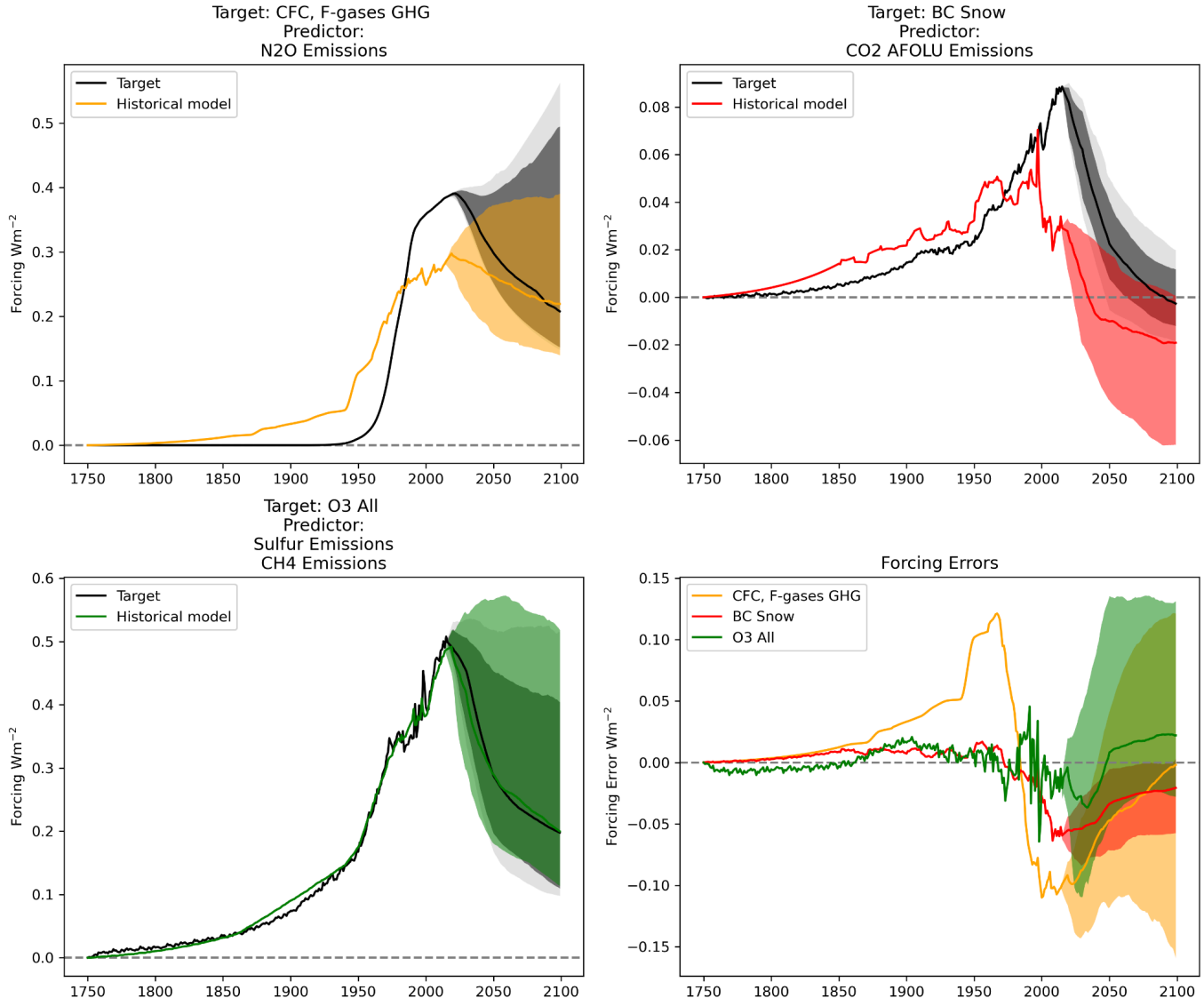

Figure 7: Three relationships between emissions within the model (Predictor) and the forcing not explicitly modelled (Target) which have been implemented in FRIDA (see text for details). The first three plots show the target forcing historically and under the future AR6 scenarios as modelled by FaIR (black), and the estimated historical and future forcing when using the chosen predictors, which are the representations implemented in FRIDA (colours). The errors for each approximation are shown in the fourth panel.

Forcing due to land-use change is modelled – as in FaIR – as a linear negative forcing from cumulative CO2 land-use emissions. In addition to these anthropogenic forcings, small solar and volcanic forcings are exogenously applied, being outside the model domain.

The total radiative forcing is input to a 3-layer energy balance model, which represents the earth system as 3 horizontal layers, with different heat capacities and thermal transfer coefficients, following Leach et al., 2021. The temperature of each layer is represented as a stock within FRIDA; the top layer receives the radiative forcing, and its temperature stock is conceptualised as the STA. At each timestep the flows of heat into the first layer and between the others, represented as temperature changes, are then calculated and added to the prior temperature stocks.

After the implementation of the differences from FaIR - primarily the modelling of certain forcings as a function of the key emitted species described above - the full set of parameters was recalibrated, with an adaptation of the approach used in FaIR to optimally match historical observations, as shown in Figure 8. FaIR uses predefined broad parameter ranges to generate 1 million possible parameter combinations, which are run in FaIR under historical conditions and a commonly-used medium-ambition future scenario (SSP245) to produce the

corresponding climate outputs. This ensemble is then reduced in two steps. First, members which don't closely reproduce historical STA (defined as an RMSE of >0.16K historically) are discarded. Then, the remaining members are reduced to produce an ensemble of several hundred parameter sets which reproduce best-estimate distributions of several climate properties: ECS, TCR, ocean heat content, STA from 1995-2014, ERFari, ERFaci, ERFaer, CO2 concentration, and estimated SSP245 STA in 2081-2100.

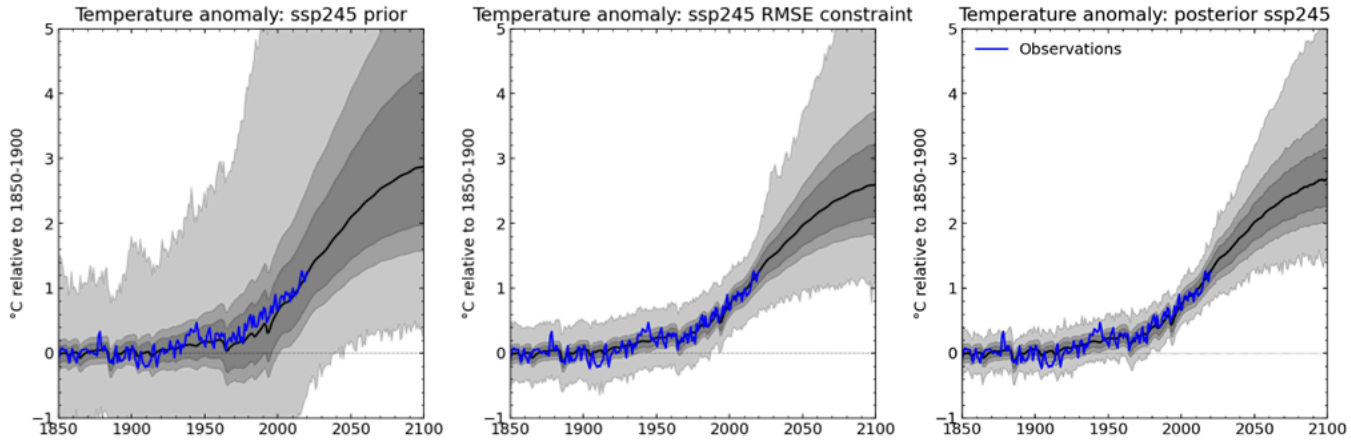

Figure 8: the 1850-2100 STA time series in FaIR of the different ensembles, using historical and SSP245 future emissions, compared to observations. The first plot indicates the full ensemble, initially constrained to reflect historical STA in the middle plot, and finally constrained to additional observations in the third plot – see text for details.

As well as generally realigning the parameter sets with observations, the recalibration accounts for specific processes which were neglected when reducing FaIR to be in FRIDA, such as non-SO2 aerosol direct and indirect effects.

Sea Level Rise

Sea level rise is one of the many consequences of a warming world. The sequence of events that result in sea level rise is complex, involving changes in runoff from land (due to changes in ground water extraction as a result of the changing demographics of the world's population), melting of glaciers and ice sheets, and expansion of the oceans themselves as they warm. Total global sea-level is modelled as the sum of five different components, which are described below. In short, the Sea-Level Rise calculation takes STA and the total radiative forcing, as well as population size as input. We explicitly simulate the individual components of SLR as the individual components can have regionally different impacts (Slangen et al., 2017), so this relatively complex formulation allows for more detailed studies and a potential regionalization of the model in the future. The possibility of future marine ice cliff instability leading to substantially increased rates of SLR is not represented by the current set of model parameters, but can easily be added in future versions of the model. In the current version of FRIDA, neither total SLR, nor the individual components are used in any other module, so currently, SLR is model output exclusively. This will change in future versions of FRIDA, where parameterizations for economic damages and adaptation costs of sea-level rise are planned to be implemented.

The five terms that sum up to total sea level are:

- Thermosteric SLR (SLR_{thermo}): The annual change of SLR_{thermo} is calculated as a linear function of the total radiative forcing as a proxy for ocean heat content. This linear relationship is shown to represent SLR_{thermo} well, and it is calibrated here using data from Earth system model simulations and IPCC estimates (Marti et al., 2022, Fox-Kemper et al., 2021).
- SLR from mountain glaciers (SLR_{MG}): The annual change of SLR_{MG} is modelled with a widely used parameterization from Wigley and Raper (2005), which depends on the STA and the cumulative contribution of this component from previous time steps. Parameter values are chosen as in Perrette et al. (2013).
- SLR from Greenland ice sheet (SLR_{GrIS}): This component is calculated based on the formulation in MAGICC6 (Nauels et al., 2017). Two different processes are considered: the surface mass balance of the

Greenland ice sheet and its discharge into the ocean, which both depend on the STA. SLR_{GrIS} is the sum of the contributions of both processes.

- SLR from Antarctic ice sheet (SLR_{AntrIS}): In FRIDA, we implement the DAIS model (Shaffer, 2014) in the version applied in the BRICK model (Wong et al., 2017). This implementation is relatively flexible and simulates the evolution of the ice sheets' radius and volume. Calibration parameters were adjusted to comply with estimates of the IPCC for the future evolution of SLR_{AntrIS} (Fox-Kemper et al., 2021). The calculation of SLR_{AntrIS} depends on the Antarctic surface ocean and air temperature - which are both parameterized from the STA - as well as on the global sea-level rise.
- SLR from land water storage (SLR_{LWS}): Since land water storage changes can be approximated as a function of population (Fox-Kemper et al., 2021, Rahmstorf et al., 2012), we obtained SLR_{LWS} through a linear regression with the dynamically evolving population within FRIDA (instead of a constant in time increase that is often implemented in other models).

4. Calibration and Behavioural Validation

A classical climate - or Earth System - model has a spatial resolution in the range of 5 to 100 km, with around fifty layers in the atmosphere and ocean. It simulates the laws of nature, and is only forced by external factors such as solar insolation, volcanic eruptions and anthropogenic actions. Climate models have to be spun up, often for several thousands of model years, to reach an equilibrium state in the atmosphere and ocean. The equilibrium state is usually chosen to be the period before large-scale anthropogenic influence, representative of year 1850 conditions. Before being used for production runs, models will often undergo calibration and tuning processes to ensure the top-of-atmosphere energy budget is approximately in balance and consistent with observations, which may require tuning of sub-grid-scale parameters (often involving convection and clouds) that cannot be explicitly resolved. A set of standard diagnostic experiments are requested from climate models that contribute to the World Climate Research Program's Coupled Model Intercomparison Project (CMIP; Eyring et al. 2016), which provides a large evidence basis to IPCC Working Group I. One diagnostic experiment is the reproduction of climate over the period of anthropogenic influence (1850 to near-present), where model performance can be compared to actual observations.

In contrast, there is limited practice in evaluating historical performance of IAMs over the anthropogenic era or of calibration to observations, though these issues have been identified (Wilson et al. 2021). The IAMs are normally based on empirical relationships built together to cover the entire economy - technology- energy nexus.

When creating simpler, box-model-type climate models (for instance Energy Balance Models), calibration towards the more complex climate models is typically performed, with observational constraints used to benchmark model performance (Leach et al. 2021). The same approach is normally used for System Dynamics models, including FRIDA. The calibration of the FRIDA model is performed both as a form of model testing, and to estimate model parameters, striving to achieve a match between the observed measurements and the simulation (Barlas, 1996, Olivia, 2003) for the time period 1980-2020 ("the calibration period"). Since changes to the model structure were needed to improve the calibration, the FRIDA model underwent a "validation / verification / calibration" process as described by Walker and Wakeland, (2011) (and briefly above).

The FRIDA model was calibrated using Powell's BOBYQA (bound optimization by quadratic approximation) (Powell, 2009), a gradient descent method. We used the version embedded in Stella Architect 3.5.1, which uses the public open source project DLib version 19.7 (Powell 2009, isee systems 2023, Dlib C++ Library 2023). FRIDA has been calibrated largely using partial calibration i.e. using 4 separate calibrations, each focused on one particular area of the model with a final whole-model calibration at the end. The 4 individual partial calibrations constructed were focused on: Economics, Population, Energy, and Food and Land Use. The Climate module was not calibrated part and parcel with the rest of the FRIDA model, instead we chose to use the published parameter estimates from the literature, since FaIR is calibrated over a longer time-period then FRIDA. This also held true for the parts of the energy module which were not modified from the MIND model which was its basis. Partial

calibration was done to reduce the computational complexity of the problem, and to allow us to bring the model into range iteratively as we worked on each portion of the model in relative isolation. This had the benefit of reducing the chance of the optimizer getting bogged down in flat areas of the payoff surface, and more importantly, made it far easier to reason about the generated parameter estimates and fits to data. For each payoff we minimised the square error between the observed data and its simulated counterpart. The weights on each component of the payoff were set so that the value of the payoff was approximately equal to the number of data points. This gives a payoff that behaves the same as the negative value of the log likelihood in terms of its response to parameter changes which is optimal for the BOBYQA algorithm. The results of FRIDA's calibration to observed data are shown in Figure 9 for all key variables identified in Figure 2.

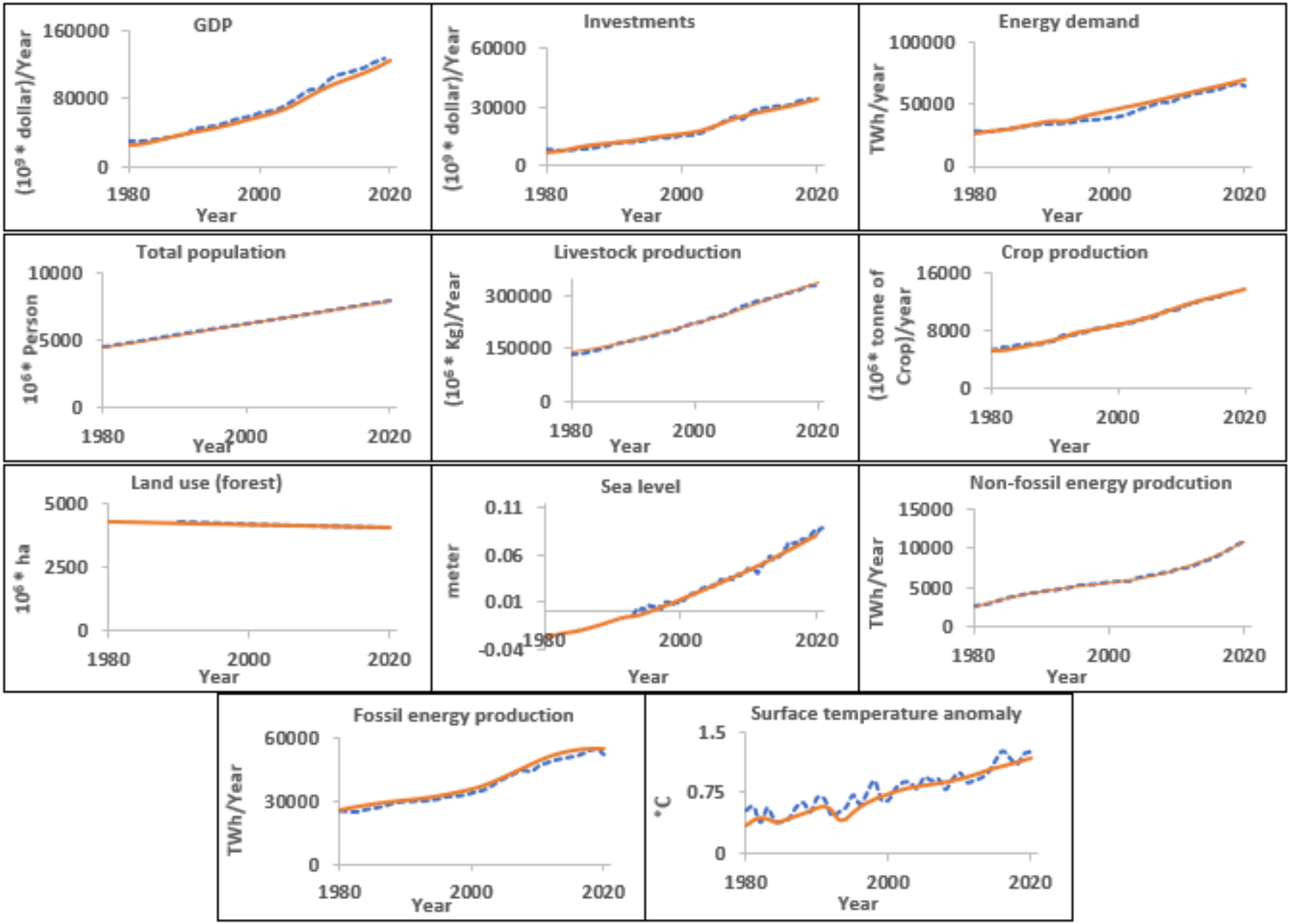

Figure 9: Calibration curves for each key variable referred to in Figure 2. The blue dashed line represents the observed data, and the solid orange line represents the simulation results. The calibration period is 1980 to 2022

5. The "Current Policies Analogy" Scenario

FRIDA's base scenario is called the "current policies analogy" scenario because it is meant to mimic the current national "policies and action" to the Paris climate agreement (Figure 10).

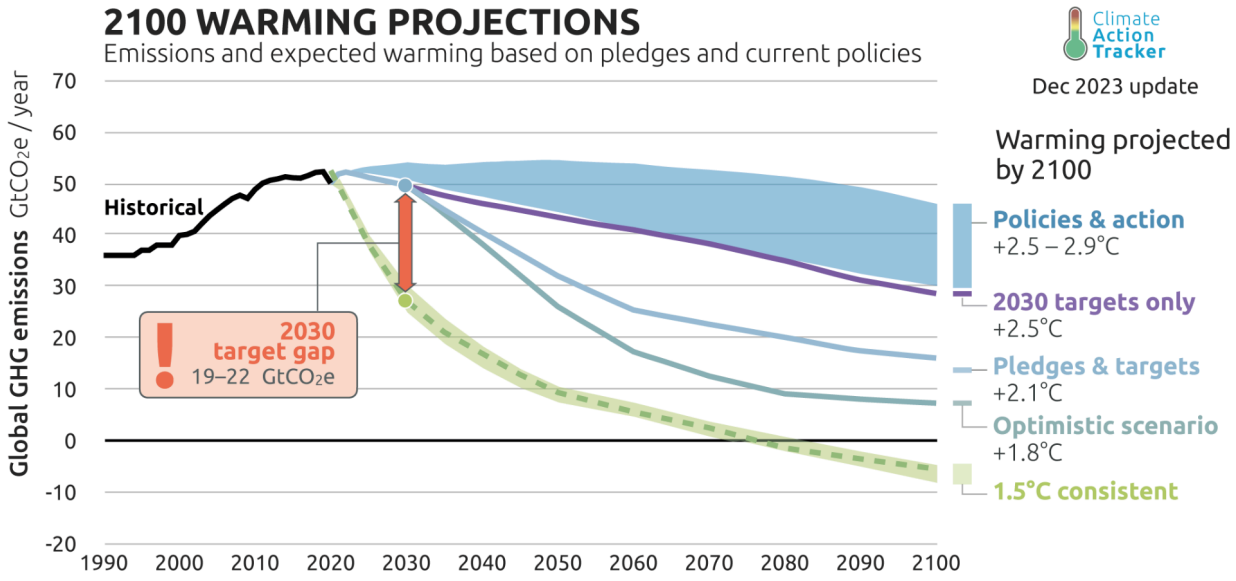

Figure 10: Climate Action Tracker warming projections, calculated using MAGIC based on national reports on emissions and pledges. This figure shows that current pledges and policies yield between 2.5℃ and 2.9℃ degrees of warming. Source: Climate Action Tracker (2023).

According to the most updated estimates (December 2023), the current policies and actions will result in a warming between 2.5 and 2.9 ℃ (Figure 10). To mimic that scenario we run FRIDA for the projection period (2020-2100) with one external intervention, namely the level of investment in renewable energy technologies relative to fossils. In FRIDA v1.0, this is an external input as the model does not yet endogenously model human decision making processes around energy type investments. For the "current policies analogy" scenario, we have chosen the energy investment strategy that best represents what is necessary to reproduce the climate outcomes of the current policies described by the Climate Action Tracker. This global energy investment strategy increases the global renewable energy supply from approximately 12% of the global energy supply in 2020, to 50% in 2040, and 97% in 2100 (Figure 11). The uncertainty bounds in this scenario (and our future policy scenarios) represent the parametric uncertainty around our six sources of climate feedback (increasing mortality, damaging energy capital, increasing energy demand, damaging crop yield, increasing water lost to evapotranspiration, and increasing failure rate of loans) in addition to the uncertainty of the climate sensitivity of FaIR. The simulation results of this scenario is shown in Figure 12.

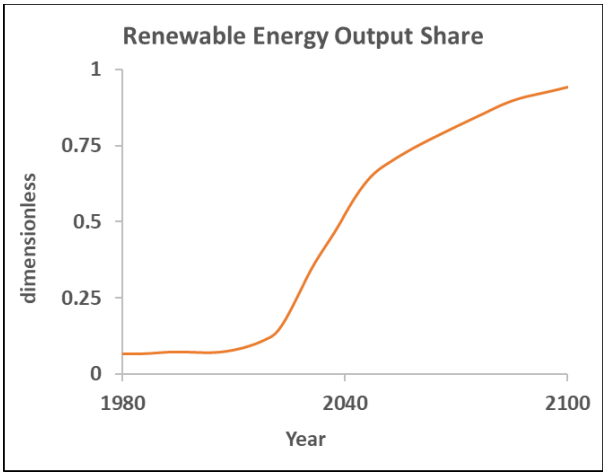

Figure 11: Renewable energy (hydro, wind, solar, and other non fossil, but not nuclear) fraction of energy supply in the "Current policies analogy" (or baseline) scenario. This is the key input to the "current policies analogy" scenario.

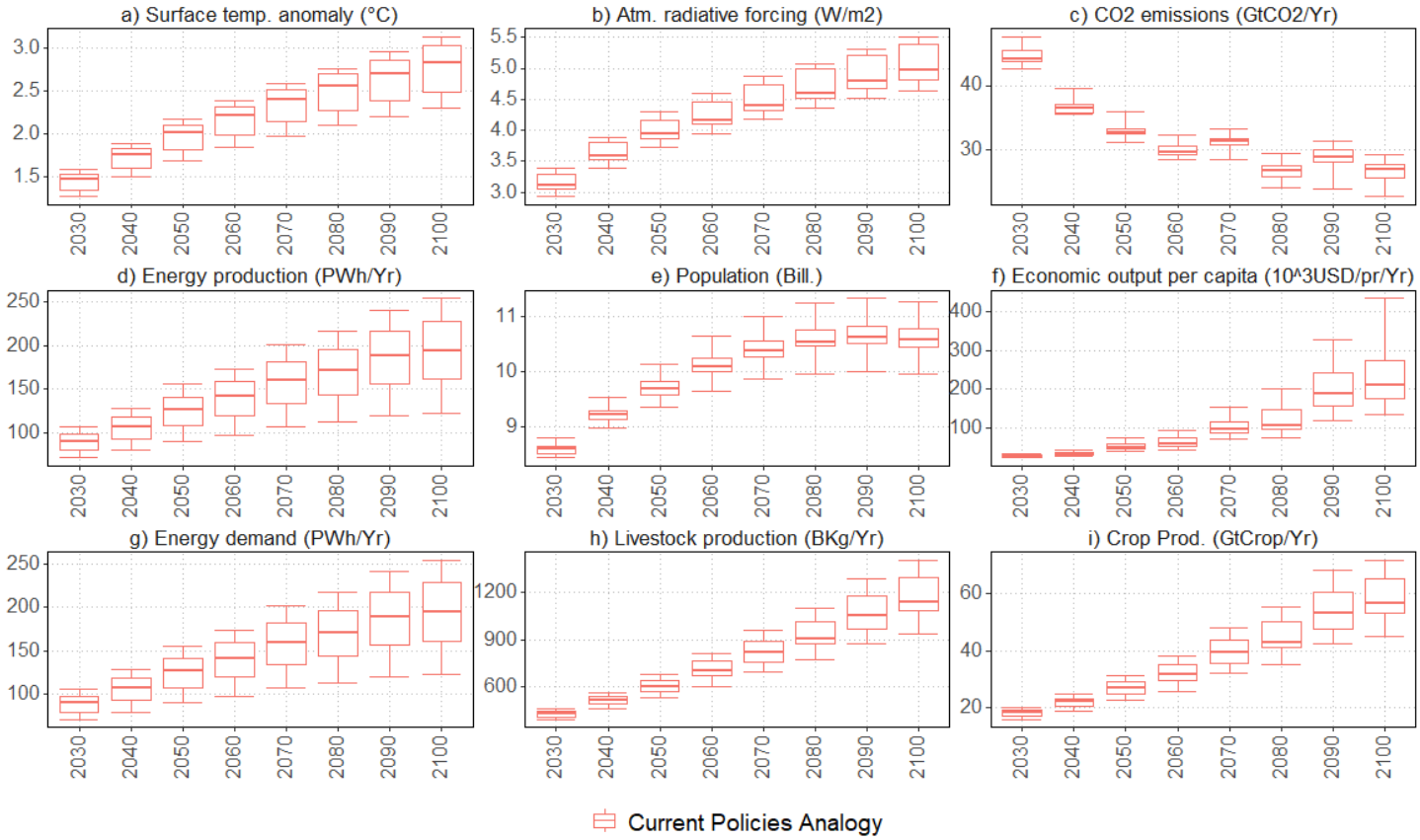

Figure 12: The baseline scenario. a) Surface temperature anomaly; b) atmospheric radiative forcing; c) CO2 emissions; d) energy production; e) population; f) economic output per capita; g) energy demand; h) livestock production; i) crop production. The uncertainty ranges show the parametric uncertainty inherent in all of the climate damage concepts within FRIDA v1.0.

The "current policies analogy" scenario projects the STA in 2100 to be 2.8℃, with an uncertainty range between 2.3℃ and 3.1℃ (Figure 12a), which by design is comparable to the "policies and action" projection in Figure 10. That level of warming is created largely by the growing concentration of GHGs in the atmosphere over the course of the century, with anthropogenic forcing in 2100 at 5.05 w/m2 (range: 4.6-5.5) (Figure 12b). In this scenario, total CO2 emissions (figure 12c) peak in the early 2030s with a maximum mean value 44.7 GtCO2/year (range: 42.6-47.8), at a level that is not all that much higher than today's emissions. The most impactful segment of emissions generating that forcing are those from energy production (Figure 12d), which are a function of the overall level of both the energy demanded by human societies and how that energy is provided (the input to the scenario). The overall amount of energy demanded, and therefore supplied to human societies, grows as a function of the increasing population (Figure 12e) and the level of economic output on a per capita basis (Figure 12f). The model projects mean energy demand in 2100 to be 195 PWh/year (range: 122-254; Figure 12g), which is just short of a threefold increase as compared to today. In the current policies analogy scenario, the human population is projected to reach a mean value in 2100 of 10.6 billion people (range: 9.96-11.3), while GDP per capita in 2100 is projected to reach a mean value of $235,000 (ppp 2017$) (range: 133,000-435,000), which is an order of magnitude increase compared to today's values. Beyond energy emissions, the increased population, and level of wealth in the absence of any specific policy interventions around consumption, generates increases in livestock production to a mean value in 2100 of 1,170 billion kg/year (range: 940-1410; Figure 12h), a roughly a three-fold increase as compared to today's levels. This increase in livestock production also increases crop production to a mean value in 2100 of 58.3 GtCrop/year (range: 45-71.8; Figure 12i), again a roughly three-fold increase as compared to today's levels. This scenario represents an interlinked world-Earth system under pressure, but most certainly not one that has collapsed.

But what would this have looked like if we hadn't included climate damages? To get an impression of the impacts that climate has on the system we present in Figure 13 the same input assumption scenario as in Figure 12, but with the following climate impacts removed: failure rate of loans, destruction of energy capital, and energy demand.

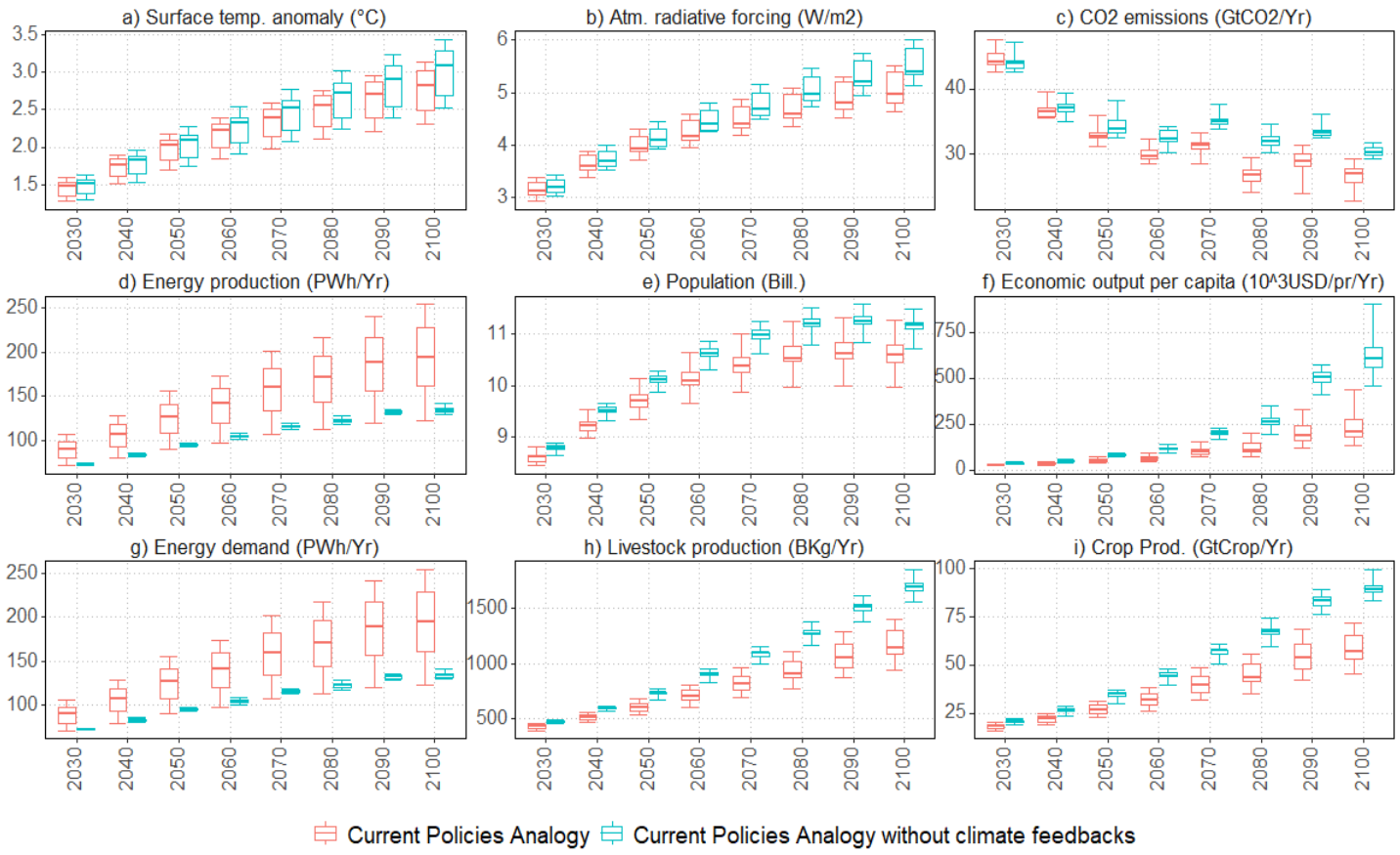

Figure 13: As in Figure 12, but with the addition of the baseline run without climate feedbacks.

In this case the warming is projected to reach 3℃ (2.5℃ - 3.4℃), which is on average one quarter degree higher than in the fully coupled model run (Figure 13a). This suggests that if the Climate Action Tracker project (Figure 10) had calculated the temperature outcomes with a model that included climate damages, the temperature projection for current policies and actions would be slightly lower! For some, this may be a rather counterintuitive result: how can climate damages cause less temperature increase? The explanation is found in the way the world develops: consider the direct outcome of the climate damage that we removed in this scenario. The first was the removal of the impact of climate on the failure rate of loans (investment) in the economic system. Without climate damage that causes loans to fail more frequently, investment returns at a higher rate, and therefore more money enters the circular flow (private sector, Figure 3). With more money entering the circular flow, both taxes and consumption increase. Since taxes form the basis for government spending, government spending also increases. Because GDP is the sum of investment, consumption and government spending, GDP increases without climate feedback (Figure 13f). That rise in GDP, lowers death rates, and combined with the insensitivity of fertility to increased economic output, at this level of GDP per capita, the removal of climate feedback drives the population up (Figure 13e). With greater economic output and higher population, there is a larger demand for meat (Figure 13h), which drives up demand for crops (Figure 13i) as well as driving up the demand and supply of energy (Figure 13d,g). All of these actions together raise total CO2 emissions (Figure 13c) which causes more anthropogenic forcing (Figure 13b) and subsequently an increase in temperature. Above we walked through just the logic behind the impacts from the removal of a single climate damage. By removing the impact of climate on the destruction of energy capital and the impact of climate on energy demand we have made it so that less investment is needed to produce energy, and that less energy is

needed (Figure 13d,g) which makes energy prices cheaper, which spurs economic growth and for the reasons above spurs additional warming.

Note that we have neither included all possible feedback in v1.0 of FRIDA, nor removed them all in the model run presented in Figure 13. What we intend to show is that the evolution of the full system is not particularly trivial to guess, and that deeper insights can be gained when considering a model that encompasses interlinkages and feedbacks of the full system, not just parts of it.

6. The impact of a heavily accelerated, unlimited, economically efficient green energy transition

The power of a fully coupled world-Earth model like FRIDA is that it allows for the quick creation of internally consistent future scenarios. As is obvious from Figure 10, current policies and actions are not enough to bring us back below 2 degree warming at the end of the century. So we have looked to FRIDA to see what it would take to bring the (FRIDA) world down below 2 degree warming.

The first scenario is based on changes in energy policies alone, and represents an extremely accelerated, and economically efficient, green energy transition. This scenario produces 85% of its energy from renewable sources in 2040, and 97% of its energy from renewable sources in 2100 (Figure 14). We obtain this by optimising investments into energy production capacity such that we maintain an energy supply demand balance of one, minimise the cost of energy production, while also minimising CO2 emissions from the energy production system, all of this assuming no materials, energy storage limitations or policy resistance.

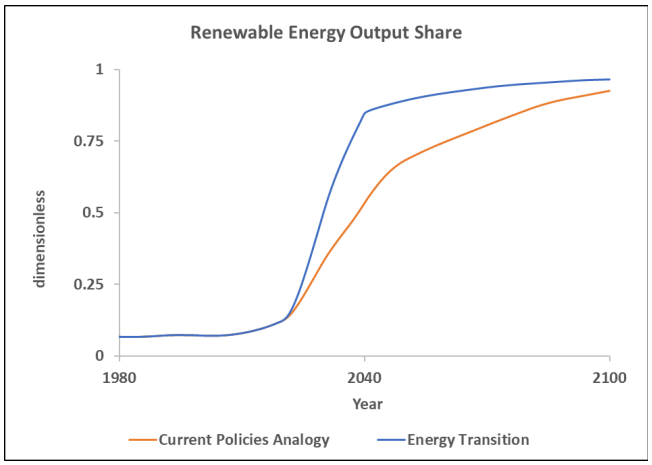

Figure 14: This figure shows the fraction of the global energy supply coming from renewable sources. The energy transition scenario input (blue) is compared to the current policies analogy scenario input (orange). The energy transition scenario sees an even more aggressive energy transition to renewable energy technologies play out. The share of renewable energy supplied to society grows far faster, and reaches a higher ultimate value in the energy transition scenario than the current policies analogy.

This energy transition scenario (depicted in Figure 15 - blue box-whiskers) is still not enough to meet a 2℃ warming goal. This scenario produces an STA in 2100 of 2.33℃ (range: 1.96-2.75), which when compared to the current policies analogy is on average a reduction of 0.42℃. The rate of growth in anthropogenic forcing is sharply reduced starting in 2040, reaching a 2100 mean that is 0.82 w/m2 less then the current policies analogy. In this scenario Total CO2 emissions peak in 2023 at a mean of 40.9 GtCO2/Year (range: 39.7-43.1), and by the end of the century emissions have steadily crept up to a mean value in 2100 of 22.3 GtCO2/year (range 17.8-26.3), though this amount is still below 1980 values. Energy demand in this scenario is only marginally different, showing on average 6 less PWh/year demanded. This change in energy demand is largely a function of the cooler climate as the global population is expected to be on average 300 million people higher in 2100 due to less impact of climate on mortality, and marginally increased levels of GDP per capita also reducing mortality. This scenario projects GDP per capita in 2100 to increase on average by $42,000 (ppp 2017$) versus the current policies analogy. These increases in population and GDP per capita have also caused livestock production to

increase on average by 100 billion kg/year in 2100, which increases crop production on average by 6 GtCrop/Year in 2100. This scenario represents a far more desirable outcome, with higher mean economic growth and overall lower temperature, but without a policy to change dietary habits, and create negative emissions through afforestation it falls short of the goal.

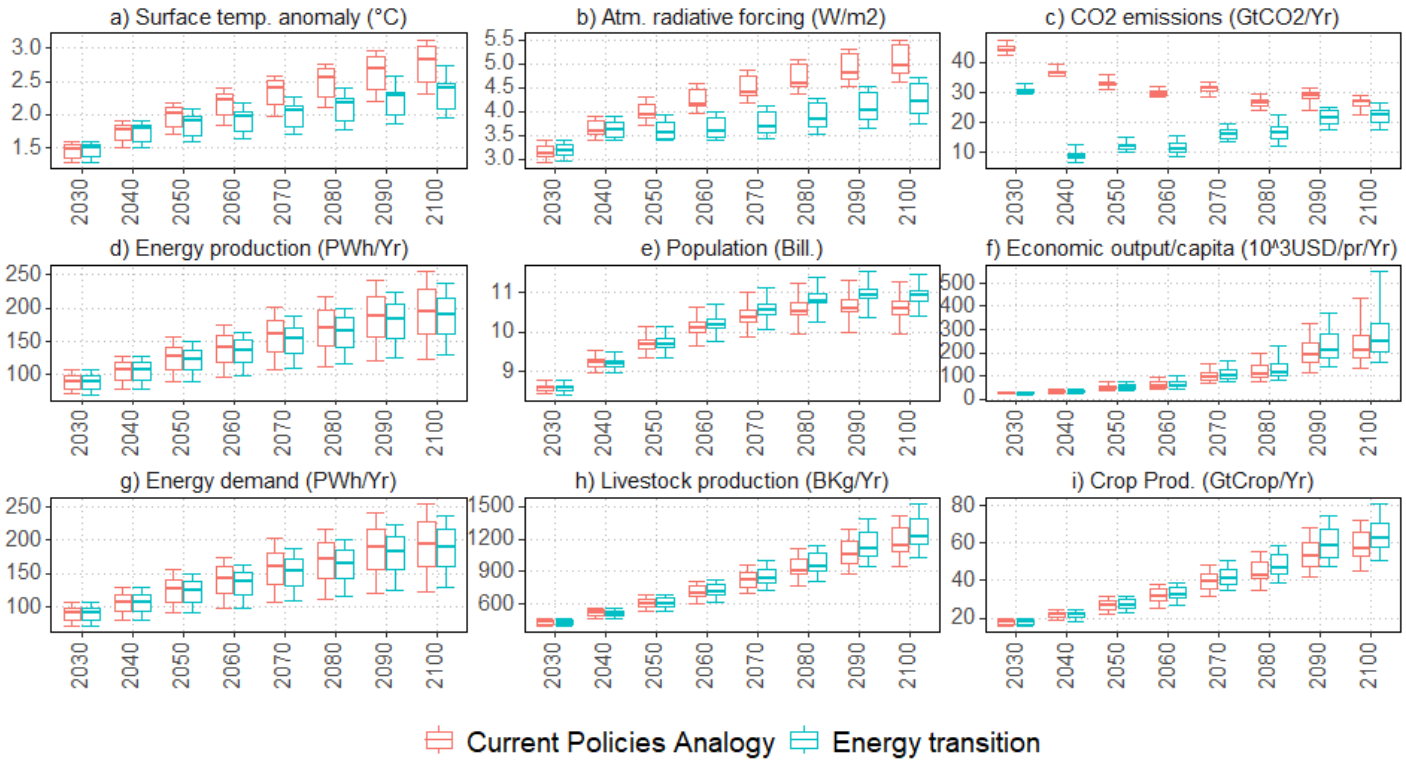

Figure 15: Results of the current policy analogy scenario (with climate feedback) compared to the energy transition scenario.

7. Afforestation and changes to livestock demand to achieve the 2 degree Celsius target

Without negative-emissions energy systems, even drastically reducing emissions from the energy system alone is not enough to get us below 2℃ warming. Finding a policy that gets us to that target without those technologies, using a fully coupled feedback-rich model (FRIDA) was surprisingly difficult. Our first intuition was to hold energy demand constant at a global level, but that had the opposite effect on STA by 2100. That happened because by 2040, with our aggressive energy transition policy, we have modelled a scenario where we are getting nearly all of our energy from renewable sources (Figure 14). Consequently, the reduction in energy demand does not significantly decrease emissions. Instead, decreasing energy demand only serves to decrease the level of investment needed to meet energy demand, allowing energy supply and demand to meet far more easily (i.e., lowering prices) and fueling additional economic growth. The additional economic growth, in turn, increases emissions from elsewhere in the system, primarily from land use, land cover changes and increased livestock production to satiate the demand for heavier meat-based diets, which is a consequence of a richer global population.

Since there are no further opportunities for reductions in emissions from the energy system, without resorting to untested at the large scale, negative emissions energy production technologies, we turned our attention to other sources of human generated emissions. We chose to focus on two primary targets: reductions in emissions from livestock production and the creation of negative CO2 emissions through afforestation. To achieve a 2℃ STA in 2100 requires the implementation of not only our energy transition described above, but also a logarithmic decay in per capita livestock demand to 1980's levels starting in 2024 (Figure 17h). The end effect of this per capita

change in livestock demand, holds livestock production roughly constant at 2020 values for the rest of the century. These two interventions together were still insufficient; they had to be done simultaneously with the yearly conversion of 1% of global grasslands to forest land starting in 2030 as seen in Figure 16.

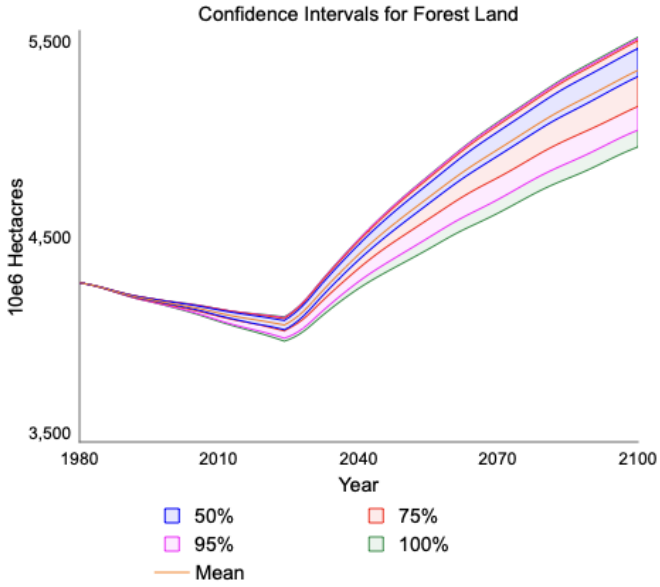

Figure 16: Impact of Afforestation Policy, restoring 1% of global grasslands to forest land each year, starting in 2030.

This scenario finally produces an STA of 2℃ (range: 1.65-2.34) in 2100. This is a reduction of 0.75℃ compared to the "current policies analogy" scenario. To achieve that reduction in temperature, anthropogenic radiative forcing (Figure 17b, green boxes) is still sharply reduced in 2040 by the energy transition (Figure 14), but in the latter half of the century it is held roughly constant (compared to slightly growing in the previous scenario), reaching a mean value in 2100 of 3.55 W/m2, which is 1.5 W/m2 less than the current policies analogy. Since forcing is the outcome of emissions, the same story holds true for total CO2 emissions, which still peak in 2023 due to the aggressive energy transition, but in this scenario the 2100 mean value is 18.2 GtCO2/year, 4.1 GtCO2/year less then even the energy transition scenario because of the afforestation policy. Energy demand is only marginally changed, showing on average 9 PWh/year less energy demand in this scenario than the energy transition scenario (Figure 17g), which is mostly due to the "cooler" climate in the latter half of the century. Population in this scenario increases relative to both the current policies analogy and the green transition scenario, reaching an average of 11.1 billion people in 2100, which is 500 million more people than the current policies analogy, and 200 million more than the green transition scenario (Figure 17e). This difference is caused both by reduced mortality from climate and marginal increases in GDP per capita, both of these pushing death rates down and, at this point in the fertility curve, fertility is very insensitive to changes in GDP per capita. GDP per capita in this scenario has a mean 2100 value of $278,000 (ppp 2017$) which is $43,000 higher than the current policies analogy, and $1,000 higher than the green transition scenario (Figure 17f). By breaking the link between GDP per capita, and livestock demand, modelling a return to 1980's levels of per capita livestock consumption, we reduce crop production on average by 12.8 GtCrop/Year compared to the current policies analogy, and 18.8 GtCrop/Year compared to the green transition scenario with its increased livestock production (Figure 17i). This scenario represents a positive outcome from the perspective of addressing climate change, without causing world-wide aggregated economic harm, based on our projections economic outcomes are generally indistinguishable in this world vs the others.

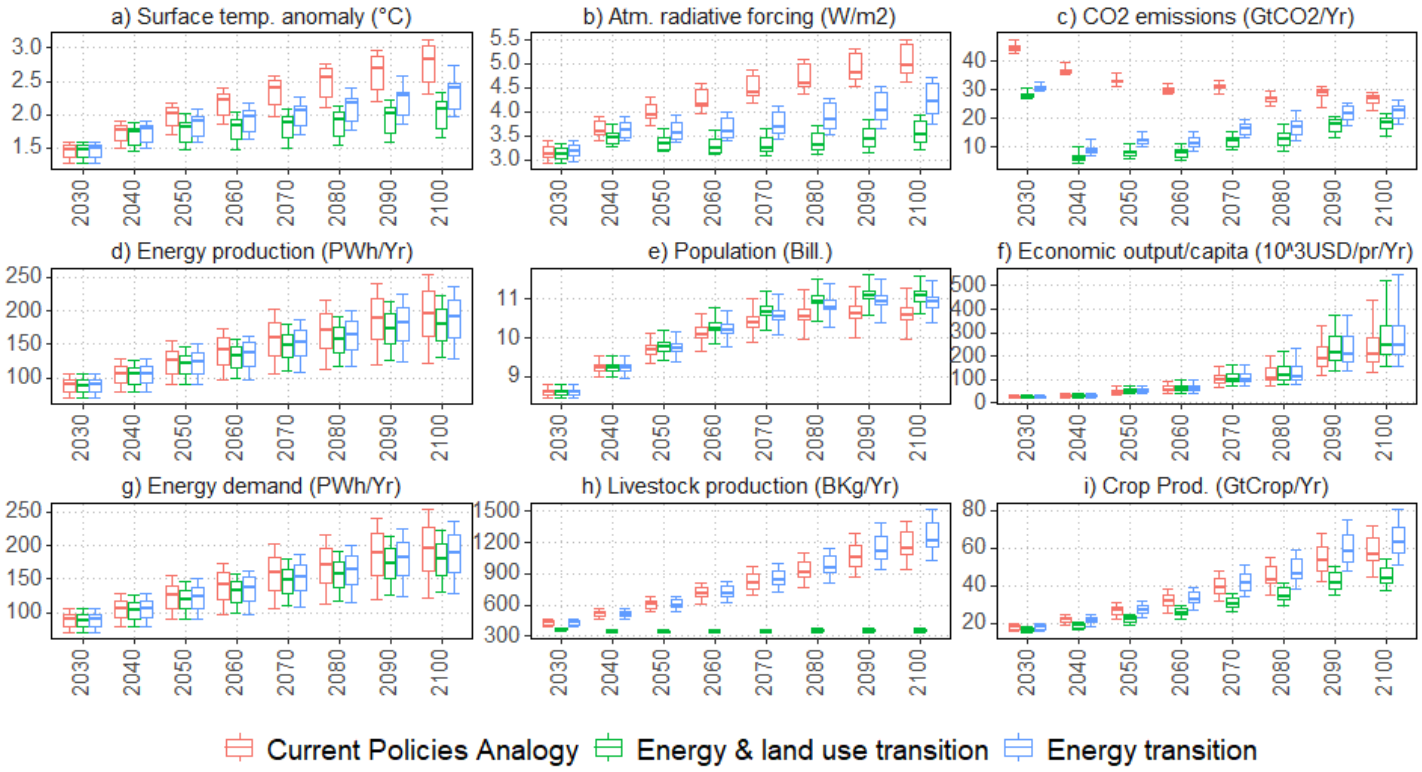

Figure 17: Results of the current policy analogy scenario (with climate feedback) in red compared to the energy transition (alone) scenario in blue and the energy & land use transition scenario necessary to reach 2℃ in green. To reach the 2℃ target in 2100 without negative emissions energy production (i.e BECCS) requires an aggressive energy transition, holding livestock production constant at today's levels, and afforestation starting in 2030.

8. Conclusions and next steps

With this work, we have demonstrated the importance of having a dynamically complex feedback-rich model which interconnects the climate and the human system. Representing the breadth of connections between the sectors of world-Earth system has allowed us to capture the unintuitive outcomes which arise from a more fully connected World Earth system, specifically that including climate damage in our model, reduces projections of warming. We have used FRIDA v1.0 (an admittedly developing model) to demonstrate the difficulty of reaching a 2℃ target in 2100 without relying on BECCS and other yet-to-be-tested at large-scale, negative emission energy producing technologies. The analysis based on this model shows that even in our most aggressive and unrealistically optimistic policy scenarios, we barely reached the 2℃ target on average. From the perspective of our developing modelling work with FRIDA v1.0, the 1.5℃ target is wholly unachievable without these negative emissions technologies, and more likely than not, 2.5℃ or warmer will be the result of current day levels of actions and commitment to addressing the causes of climate change.

The FRIDA model, presented here, is only a step on a journey towards achieving our goals of developing a new combined climate-IAM that is fully transparent and has a strong social and human component. We have demonstrated that FRIDA is a potentially plausible model of the development of human society and the Earth's climate over the past 40 and next 80 years. While we have explored many of the interconnections between the climate and human society, there is still more work to be done. Moving forward to FRIDA v2.0 will require a focus on modelling human behaviour in a more direct and explicit way in all modules, allowing us to refine our scenario creation process, avoiding outcomes which are unrealistic and creating stories and scenarios that are "fit for purpose". Across the entire model we need to add more detail to the carbon cycle and water cycles. To the energy and industries system, we would like to integrate the limitations to the energy transition from resources (i.e., rare earth metals etc.) and better disaggregate the supply and demand of energy by the type of demand

(transport, heating, etc.). To the economy, we would like to add structure to represent more aspects of the economy - for instance the concept of inequality - to test and see if our projections of future economic growth hold up as we make the economy less financialized. To the food and land use system, we would like to add the ability to simulate BECCS. We also would like to ground the existing representation of climate impacts more solidly within existing literature, and add further types of climate damage. Our hope is that FRIDA will soon be at a level mature enough to address many of the serious questions concerning climate that are facing the world with enough confidence to be heard.

Acknowledgements

This work was supported by the Horizon Europe project WorldTrans which has received funding from the European Union's Horizon 2.5 - Climate Energy and Mobility programme under grant agreement No. 10108166.

References

Asea, P. K., & Blomberg, B. 1998. Lending cycles. Journal of Econometrics, 83(1-2), 89-128. https://doi.org/10.1016/S0304-4076(97)00066-3

Barlas Y. 1996. Formal aspects of model validity and validation in system dynamics. System Dynamics Review: The Journal of the System Dynamics Society 12(3): 183-210. https://doi.org/10.1002/(SICI)1099-1727(199623)12:3<183::AID-SDR103>3.0.CO;2-4

Bolt J, Van Zanden JL. 2020. Maddison style estimates of the evolution of the world economy. A new 2020 update. Maddison-Project Working Paper WP-15, University of Groningen, Groningen, The Netherlands. Available at: https://www.rug.nl/ggdc/historicaldevelopment/maddison/releases/maddison-project-database-2020

Breier, J. 2023. Regionalisation of FAO & Hyde data (Version 0.1.0) [Computer software]. https://github.com/github/linguist

Budischak, C., Sewell, D., Thomson, H., Mach, L., Veron, D.E. and Kempton, W., 2013. Cost-minimized combinations of wind power, solar power and electrochemical storage, powering the grid up to 99.9% of the time. journal of power sources, 225, pp.60-74. https://doi.org/10.1016/j.jpowsour.2012.09.054

Byers E., Krey V., Kriegler E., Riahi K., Schaeffer R., Kikstra J., Lamboll R., Nicholls Z., Sandstad M., Smith C., van der Wijst K., 2022. AR6 Scenarios Database hosted by IIASA International Institute for Applied Systems Analysis, 2022. doi: 10.5281/zenodo.5886911

Calvin K., Bond-Lamberty B. 2018. Integrated human-Earth system modeling—State of the science and future directions. Environmental Research Letters 13(6). doi:10.1088/1748-9326/aac642

Chinowsky P, Arndt C. 2012: Climate Change and Roads: A Dynamic Stressor-Response Model. Review of Development Economics 16(3): 448–462. doi:10.1111/j.1467-9361.2012.00673.x.

Climate Action Tracker (2023). 2030 Emissions Gap: CAT projections and resulting emissions gap in meeting the 1.5°C Paris Agreement goal. December 2023. Available at: https://climateactiontracker.org/global/cat-emissions-gaps/. Copyright ©2023 by Climate Analytics and NewClimate Institute. All rights reserved.

Copernicus climate change service (C3S) (2023), https://marine.copernicus.eu/ocean-climate-portal/sea-level

Dell'Ariccia, G., & Marquez, R. 2006. Lending booms and lending standards. The journal of finance, 61(5), 2511-2546. https://doi.org/10.1111/j.1540-6261.2006.01065.x

Dentener FJ, Hall B, Smith C. 2021. IPCC, 2021: Annex III: Tables of historical and projected well-mixed greenhouse gas mixing ratios and effective radiative forcing of all climate forcers. In Climate Change 2021: The Physical Science Basis. Contribution of Working Group I to the Sixth Assessment Report of the Intergovernmental Panel on Climate Change, 590.

Dlib C++ Library. 2023. Available at: http://dlib.net/

Eberlein RL, Thompson JP. 2013. Precise modeling of aging populations. System Dynamics Review 29(2):87-101. https://doi.org/10.1002/sdr.1497

Edenhofer, O., Bauer, N. and Kriegler, E., 2005. The impact of technological change on climate protection and welfare: Insights from the model MIND. Ecological economics, 54(2-3), pp.277-292. https://doi.org/10.1016/j.ecolecon.2004.12.030

Edgerton MD. 2009. Increasing crop productivity to meet global needs for feed, food, and fuel. Plant Physiol 149(1): 7-13. doi: 10.1104/pp.108.130195. https://doi.org/10.1104/pp.108.130195

Eker S, Reese G, Obersteiner M. 2019. Modelling the drivers of a widespread shift to sustainable diets. Nature Sustainability 2(8): 725–735. https://doi.org/10.1038/s41893-019-0331-1

Energy Institute - Statistical Review of World Energy (2023). https://www.energyinst.org/statistical-review

EPA, 2017: Inventory of U.S. Greenhouse Gas Emissions and Sinks 1990-2015.

Espinet, X., Schweikert, A., van den Heever, N. and Chinowsky, P., 2016. Planning resilient roads for the future environment and climate change: Quantifying the vulnerability of the primary transport infrastructure system in Mexico. Transport Policy, 50, pp.78-86. https://doi.org/10.1016/j.tranpol.2016.06.003

Eyring, V., Bony, S., Meehl, G.A., Senior, C.A., Stevens, B., Stouffer, R.J. and Taylor, K.E., 2016. Overview of the Coupled Model Intercomparison Project Phase 6 (CMIP6) experimental design and organization. Geoscientific Model Development, 9(5), pp.1937-1958. https://doi.org/10.5194/gmd-9-1937-2016

Feenstra RC, Inklaar R, Timmer MP. 2015. The Next Generation of the Penn World Table. American Economic Review 105(10): 3150-3182. DOI: 10.1257/aer.20130954, available for download at www.ggdc.net/pwt

Feenstra RC, Inklaar R, Timmer MP. 2015. The Next Generation of the Penn World Table. American Economic Review 105(10): 3150-3182. DOI: 10.1257/aer.20130954, available for download at www.ggdc.net/pwt

Forouzbakhsh, F., Hosseini, S.M.H. and Vakilian, M., 2007. An approach to the investment analysis of small and medium hydro-power plants. Energy Policy, 35(2), pp.1013-1024. https://doi.org/10.1016/j.enpol.2006.02.004

Food and Agriculture Organization (FAO) (January 2023) Data. Available at: https://www.fao.org/home/en

Ford A. 2010. Modeling the Environment (Second Edition ed.). Washington, DC: Island Press.

Forrester, J.W., 1961. Industrial dynamics mit press cambridge. MA.[Google Scholar].

Forrester, J.W. 1971: World Dynamics. Wright-Allen Press, Cambridge, Massachusetts.

Forrester, J.W., 1994. System dynamics, systems thinking, and soft OR. System dynamics review, 10(2‐3), pp.245-256. https://doi.org/10.1002/sdr.4260100211

Forster P, Storelvmo T, Armour K, Collins W, Dufresne JL, Frame D. et al. 2021. The Earth's Energy Budget, Climate Feedbacks, and Climate Sensitivity. In Climate Change 2021: The Physical Science Basis. Contribution of Working Group I to the Sixth Assessment Report of the Intergovernmental Panel on Climate Change.

Fox-Kemper, B., H.T. Hewitt, C. Xiao, G. Aðalgeirsdóttir, S.S. Drijfhout, T.L. Edwards, N.R. Golledge, M. Hemer, R.E. Kopp, G. Krinner, A. Mix, D. Notz, S. Nowicki, I.S. Nurhati, L. Ruiz, J.-B. Sallée, A.B.A. Slangen, and Y. Yu, 2021: Ocean, Cryosphere and Sea Level Change. In Climate Change 2021: The Physical Science Basis. Contribution of Working Group I to the Sixth Assessment Report of the Intergovernmental Panel on Climate Change [Masson-Delmotte, V., P. Zhai, A. Pirani, S.L. Connors, C. Péan, S. Berger, N. Caud, Y. Chen, L. Goldfarb, M.I. Gomis, M. Huang, K. Leitzell, E. Lonnoy, J.B.R. Matthews, T.K. Maycock, T. Waterfield, O. Yelekçi, R. Yu, and B. Zhou (eds.)]. Cambridge University Press, Cambridge, United Kingdom and New York, NY, USA, pp. 1211–1362, doi:10.1017/9781009157896.011.

Friedlingstein P, Cox P, Betts R, Bopp L, von Bloh W, Brovkin V, Cadule P, Doney S, Eby M, Fung I, Bala G. 2006. Climate–carbon cycle feedback analysis: results from the C4MIP model intercomparison. Journal of climate 19(14): 3337-3353. https://doi.org/10.1175/JCLI3800.1

Friedlingstein P, O'Sullivan M, Jones MW, Andrew R M, Gregor L, Hauck J, Le Quéré C, Luijkx IT, Olsen, A., Peters GP, Peters W, Pongratz J, Schwingshackl C, Sitch S, Canadell JG, Ciais P, Jackson RB, Alin SR, Alkama R, Arneth A, Arora VK, Bates NR, Becker M, Bellouin N, Bittig H C, Bopp L, Chevallier F, Chini LP, Cronin M, Evans W, Falk S, Feely RA, Gasser T, Gehlen M, Gkritzalis T, Gloege L, Grassi G, Gruber N, Gürses Ö, Harris I, Hefner M, Houghton RA, Hurtt GC, Iida Y, Ilyina T, Jain AK, Liu Z, Marland G, Mayot N, McGrath MJ, Metzl N, Monacci NM, Munro DR, Nakaoka SI, Niwa Y, O'Brien K, Ono T, Palmer PI, Pan N, Pierrot D, Pocock K, Poulter B, Resplandy L, Robertson E, Rödenbeck C, Rodriguez C, Rosan TM, Schwinger J, Séférian R, Shutler JD, Skjelvan I, Steinhoff T, Sun Q, Sutton AJ, Sweeney C, Takao S, Tanhua T, Tans P P, Tian X, Tian H, Tilbrook B, Tsujino H, Tubiello F, van der Werf GR, Walker AP, Wanninkhof R, Whitehead C, Willstrand Wranne A, Wright R, Yuan W, Yue C, Yue X, Zaehle S, Zeng J, Zheng B. 2022. Global Carbon Budget , Earth System Science Data 14: 4811-4900. https://doi.org/10.5194/essd-14-4811-2022

Global International Geosphere-Biosphere Programme (IGB), http://www.igbp.net/

Global Trends in Renewable Energy Investment 2020, United Nations Environment Programme, Frankfurt School of Finance and Management, BloombergNEF, 2020, https://wedocs.unep.org/20.500.11822/32700

Hayward, J.A., Graham, P.W. and Campbell, P.K., 2011. Projections of the future costs of electricity generation technologies: an application of CSIRO's Global and Local Learning Model (GALLM). EP104982: CSIRO.

Held, H., Kriegler, E., Lessmann, K. and Edenhofer, O., 2009. Efficient climate policies under technology and climate uncertainty. Energy Economics, 31, pp.S50-S61.https://doi.org/10.1016/j.eneco.2008.12.012

Hsiang, S. and Sekar, N., 2016. Does legalization reduce black market activity? Evidence from a global ivory experiment and elephant poaching data (No. w22314). National Bureau of Economic Research. DOI 10.3386/w22314.

International Atomic Energy Agency, 2023, https://www.iaea.org/

International Energy Agency (IEA) 2022, Installed power generation capacity by source in the Stated Policies Scenario, 2000-2040, viewed in January 2023. Available at: https://www.iea.org/data-and-statistics/charts/installed-power-generation-capacity-by-source-in-the-stated-policies-scenario-2000-2040

International Energy Agency (IEA) World Energy Investment 2023, https://www.iea.org/

International Labour Organization, Labour share of GDP (%), 2022. https://ilostat.ilo.org/

International Labour Organization. "ILO Modelled Estimates and Projections database (ILOEST)" ILOSTAT. Accessed February 21, 2023. ilostat.ilo.org/data.

International Renewable Energy Agency (2023) – processed by Our World in Data. "Global installed renewable energy capacity by technology" [dataset]. International Renewable Energy Agency, "Renewable Electricity Capacity and Generation Statistics" [original data]. Retrieved March 14, 2024 from https://ourworldindata.org/grapher/installed-global-renewable-energy-capacity-by-technology

International Renewable Energy Agency (IRENA) 2022, https://www.irena.org/Statistics/Download-query-tools.

Isee Systems, 2023. https://iseesystems.com

Donges, J.F., Lucht, W., Heitzig, J., Barfuss, W., Cornell, S.E., Lade, S.J. and Schlüter, M., 2018. Taxonomies for structuring models for World-Earth system analysis of the Anthropocene: subsystems, their interactions and social-ecological feedback loops. Earth System Dynamics Discussions, 2018, pp.1-30. https://doi.org/10.5194/esd-12-1115-2021

Karstens, K., Bodirsky, B.L., Dietrich, J.P., Dondini, M., Heinke, J., Kuhnert, M., Müller, C., Rolinski, S., Smith, P., Weindl, I. and Lotze-Campen, H., 2020. Management induced changes of soil organic carbon on global croplands. Biogeosciences Discussions, 2020, pp.1-30. https://doi.org/10.5194/bg-19-5125-2022

Kimball BA, Idso SB. 1983. Increasing atmospheric CO2: effects on crop yield, water use and climate. Agricultural water management 7(1-3): 55-72. https://doi.org/10.1016/0378-3774(83)90075-6

King, R.G. and Levine, R., 1993. Finance and growth: Schumpeter might be right. The quarterly journal of economics, 108(3), pp.717-737.https://doi.org/10.2307/2118406

Kirk D. 1996. Demographic transition theory. Population Studies 50(3): 361–387. https://doi.org/10. 1080/0032472031000149536.

Kwakkel, J.H., Walker, W.E. and Marchau, V.A., 2010. Classifying and communicating uncertainties in model-based policy analysis. International journal of technology, policy and management, 10(4), pp.299-315. https://doi.org/10.1504/IJTPM.2010.036918

Lal, R. (2004). Soil carbon sequestration impacts on global climate change and food security. *science*, *304*(5677), 1623-1627. https://doi.org/10.1126/science.1097396

Lal, R., Negassa, W., & Lorenz, K. (2015). Carbon sequestration in soil. Current Opinion in Environmental Sustainability, 15, 79-86. https://doi.org/10.1016/j.cosust.2015.09.002

Lambin EF, Meyfroidt P. 2011. Global land use change, economic globalization, and the looming land scarcity. Proceedings of the national academy of sciences 108(9): 3465-3472. https://doi.org/10.1073/pnas.1100480108

Leach NJ, Jenkins S, Nicholls Z, Smith CJ, Lynch J, Cain M, Walsh T, Wu B, Tsutsui J, Allen MR. 2021. FaIRv2. 0.0: a generalized impulse response model for climate uncertainty and future scenario exploration. Geoscientific Model Development 14(5): 3007-3036. https://doi.org/10.5194/gmd-14-3007-2021

Lesthaeghe, R. 2010. The unfolding story of the second demographic transition. Population and Development Review 36(2): 211–251. https://doi.org/10.1111/j.1728-4457.2010.00328.x

Loayza, N.V. and Ranciere, R., 2006. Financial development, financial fragility, and growth. Journal of money, credit and banking, pp.1051-1076.

Long, S.P., Ainsworth, E.A., Leakey, A.D., Nosberger, J. and Ort, D.R., 2006. Food for thought: lower-than-expected crop yield stimulation with rising CO2 concentrations. science, 312(5782), pp.1918-1921. https://doi.org/10.1126/science.1114722

Mar, K.A., Unger, C., Walderdorff, L. and Butler, T., 2022. Beyond CO2 equivalence: The impacts of methane on climate, ecosystems, and health. Environmental science & policy, 134, pp.127-136. https://doi.org/10.1016/j.envsci.2022.03.027

Marle, M.V., Kloster, S., Magi, B.I., Marlon, J.R., Daniau, A.L., Field, R.D., Arneth, A., Forrest, M., Hantson, S., Kehrwald, N.M. and Knorr, W., 2017. Historic global biomass burning emissions for CMIP6 (BB4CMIP) based on merging satellite observations with proxies and fire models (1750–2015). Geosci. Model Dev., 10, pp.3329-3357. https://doi.org/10.5194/gmd-10-3329-2017

Marquez-Ramos L, Mourelle E. 2019. Education and economic growth: an empirical analysis of nonlinearities", Applied Economic Analysis 27 (79): 21-45. https://doi.org/10.1108/AEA-06-2019-0005

Marti, F., Blazquez, A., Meyssignac, B., Ablain, M., Barnoud, A., Fraudeau, R., Jugier, R., Chenal, J., Larnicol, G., Pfeffer, J., Restano, M., and Benveniste, J. 2022. Monitoring the ocean heat content change and the Earth energy imbalance from space altimetry and space gravimetry, Earth Syst. Sci. Data, 14, 229–249,

https://doi.org/10.5194/essd-14-229-2022

Masson-Delmotte V, Zhai P, Pirani A, Connors SL, Péan C, Berger S, Caud N, Chen Y, Goldfarb L, Gomis MI, Huang M. 2021. IPCC, 2021: Climate Change 2021: The Physical Science Basis. Contribution of Working Group I to the Sixth Assessment Report of the Intergovernmental Panel on Climate Change, 2. Cambridge University Press, Cambridge, United Kingdom and New York, NY, USA, 2391 pp. doi:10.1017/9781009157896

Meadows, D., Randers, J. and Meadows, D., 2004. A synopsis: Limits to growth: The 30-year update. Estados Unidos: Chelsea Green Publishing Company, 381.

Meadows DH, Meadows DL, Randers J. 1993. Beyond the Limits: An Executive Summary. Bulletin of Science, Technology & Society 13(1): 3–14. https://doi.org/10.1177/027046769301300102

Meadows, D.H., Randers, J. and Meadows, D.L., 2013. The limits to growth (1972). In The future of nature (pp. 101-116). Yale University Press. https://doi.org/10.12987/9780300188479-012

Meadows, D.L., Behrens, W.W., Meadows, D.H., Naill, R.F., Randers, J. and Zahn, E., 1974. Dynamics of growth in a finite world (Vol. 360). Cambridge, MA: Wright-Allen Press.

Meinshausen M, Nicholls ZR, Lewis J, Gidden MJ, Vogel E, Freund M, Beyerle U, Gessner C, Nauels A, Bauer N, Canadell JG. 2020. The shared socio-economic pathway (SSP) greenhouse gas concentrations and their extensions to 2500. Geoscientific Model Development 13(8):3571-605. https://doi.org/10.5194/gmd-13-3571-2020

Miladinov, G. 2020. Socioeconomic development and life expectancy relationship: evidence from the EU accession candidate countries. Genus 76 (2). https://doi.org/10.1186/s41118-019-0071-0

Moss RH, Edmonds JA, Hibbard KA, Manning MR, Rose SK, Van Vuuren DP, Carter TR, Emori S, Kainuma M, Kram T, Meehl GA. 2010. The next generation of scenarios for climate change research and assessment. Nature 463: 747–756. https://doi.org/10.1038/nature08823

NASA 1988. Earth System Science: A Closer View (The Bretherton Report). National Academies Press. https://doi.org/10.17226/19088

Nauels, A., Meinshausen, M., Mengel, M., Lorbacher, K., and Wigley, T. M. L. 2017. Synthesizing long-term sea level rise projections – the MAGICC sea level model v2.0, Geosci. Model Dev., 10, 2495–2524, https://doi.org/10.5194/gmd-10-2495-2017

Nicholls Z, Meinshausen M, Lewis J, Corradi MR, Dorheim K, Gasser T, Gieseke R, Hope AP, Leach NJ, McBride LA, Quilcaille Y. 2021. Reduced complexity Model Intercomparison Project Phase 2: Synthesizing Earth system knowledge for probabilistic climate projections. Earth's Future 9:6, e2020EF001900. https://doi.org/10.1029/2020EF001900

Nicholls Z, Meinshausen M, Lewis J, Corradi MR, Dorheim K, Gasser T, Gieseke R, Hope AP, Leach NJ, McBride LA, Quilcaille Y. 2021. Reduced complexity Model Intercomparison Project Phase 2: Synthesizing Earth system knowledge for probabilistic climate projections. Earth's Future 9:6, e2020EF001900. https://doi.org/10.1029/2020EF001900

Nicholls, ZR, Meinshausen M, Lewis J, Gieseke R, Dommenget D, Dorheim K, Fan CS, Fuglestvedt JS, Gasser T, Golüke U, Goodwin P. 2020. Reduced Complexity Model Intercomparison Project Phase 1: introduction and evaluation of global-mean temperature response. Geoscientific Model Development 13(11): 5175-5190. https://doi.org/10.5194/gmd-13-5175-2020

Nikiforos, M. and Zezza, G., 2018. Stock‐flow consistent macroeconomic models: A survey. Analytical Political Economy, pp.63-102. https://doi.org/10.1002/9781119483328.ch4

O'Neill, B.C., Carter, T.R., Ebi, K., Harrison, P.A., Kemp-Benedict, E., Kok, K., Kriegler, E., Preston, B.L., Riahi, K., Sillmann, J. and van Ruijven, B.J., 2020. Achievements and needs for the climate change scenario framework. Nature climate change, 10(12), pp.1074-1084. https://doi.org/10.1038/s41558-020-00952-0

Oliva R. 2003. Model calibration as a testing strategy for system dynamics models. European Journal of Operational Research 151(3):552-68. https://doi.org/10.1016/S0377-2217(02)00622-7

Perrette, M., Landerer, F., Riva, R., Frieler, K., and Meinshausen, M. 2013. A scaling approach to project regional sea level rise and its uncertainties, Earth Syst. Dynam., 4, 11–29, https://doi.org/10.5194/esd-4-11-2013

Powell MJ. 2009. The BOBYQA algorithm for bound constrained optimization without derivatives. Cambridge NA Report NA2009/06, University of Cambridge, Cambridge, 26.

Power Reactor Information System (PRIS) 2023, Nuclear Power Capacity Trend, viewed January 2023. https://pris.iaea.org/pris/Home.aspx

Prather, M.J., Hsu, J., DeLuca, N.M., Jackman, C.H., Oman, L.D., Douglass, A.R., Fleming, E.L., Strahan, S.E., Steenrod, S.D., Søvde, O.A. and Isaksen, I.S., 2015. Measuring and modeling the lifetime of nitrous oxide including its variability. Journal of Geophysical Research: Atmospheres, 120(11), pp.5693-5705. https://doi.org/10.1002/2015JD023267

Proto E, Rustichini A. 2013. A reassessment of the relationship between GDP and life satisfaction. PLoS One 8(11):e79358. doi: 10.1371/journal.pone.0079358.

Pörtner HO, Roberts DC, Adams H, Adler C, Aldunce P, Ali E, Begum RA, Betts R, Kerr RB, Biesbroek R, Birkmann J. 2022. IPCC, 2022: Climate Change 2022. Impacts, Adaptation, and Vulnerability. Contribution of Working Group II to the Sixth Assessment Report of the Intergovernmental Panel on Climate Change. Cambridge University Press, Cambridge, UK and New York, NY, USA, 3056 pp., doi:10.1017/9781009325844.

Rahmstorf, S., Perrette, M., Vermeer, M. 2012. Testing the robustness of semi-empirical sea level projections. Climate Dynamics 39, 861-875. https://doi.org/10.1007/s00382-011-1226-7

Ranasinghe R, Ruane AC, Vautard R, Arnell N, Coppola E, Cruz FA, Dessai S, Saiful Islam AKM, Rahimi M, Carrascal DR, Sillmann J. 2021. Climate Change Information for Regional Impact and for Risk Assessment. In Climate Change 2021: The Physical Science Basis. Contribution of Working Group I to the Sixth Assessment Report of the Intergovernmental Panel on Climate Change. Cambridge University Press, Cambridge, United Kingdom and New York, NY, USA, pp. 1767–1926, doi: 10.1017/9781009157896.014.

Riahi K, Schaeffer R, Arango J, Calvin K, Guivarch C, Hasegawa T, Jiang K, Kriegler E, Matthews R, Peters GP, Rao A. 2022. Mitigation of Climate Change. Contribution of Working Group III to the Sixth Assessment Report of the Intergovernmental Panel on Climate Change. Cambridge University Press, Cambridge, UK and New York, NY, USA. doi: 10.1017/9781009157926.005

Riahi K, Van Vuuren DP, Kriegler E, Edmonds J, O'neill BC, Fujimori S, Bauer N, Calvin K, Dellink R, Fricko O, Lutz W. 2017. The Shared Socioeconomic Pathways and their energy, land use, and greenhouse gas emissions implications: An overview. Global environmental change 42: 153-168. https://doi.org/10.1016/j.gloenvcha.2016.05.009

Rogelj J, Popp A, Calvin K, Luderer G, Emmerling J, Gernaat D. 2018. Scenarios towards limiting climate change below 1.5◦ C. Nature Climate Change 8 (4): 325-332. doi:10.1038/s41558-018-0091-3.

Rosvold EL, Buhaug H. 2021. GDIS, a Global Dataset of Geocoded Disaster Locations. Sci. Data 8:61. https://doi.org/10.1038/s41597-021-00846-6

Rydzak F., Obersteiner M., Kraxner F., Fritz S., McCallum I. 2013. FeliX3–Impact Assessment Model: Systemic view across Societal Benefit Areas beyond Global Earth Observation. Laxenburg: International Institute for Applied Systems Analysis (IIASA).

Saltelli, A., Ratto, M., Andres, T., Campolongo, F., Cariboni, J., Gatelli, D., Saisana, M. and Tarantola, S., 2008. Global sensitivity analysis: the primer. John Wiley & Sons.

Schaeffer R, Szklo AS, de Lucena AFP, Borba BSMC, Nogueira LPP, Fleming FP, Troccoli A, Harrison M, Boulahya MS. 2012. Energy sector vulnerability to climate change: A review. Energy 38(1): 1–12, doi:10.1016/j.energy.2011.11.056

Schlissel, D. and Bruce, B., 2008. Nuclear power plant construction costs (Synapse Energu Economics Inc.).

Shaffer, G. 2014. Formulation, calibration and validation of the DAIS model (version 1), a simple Antarctic ice sheet model sensitive to variations of sea level and ocean subsurface temperature, Geosci. Model Dev., 7, 1803–1818, https://doi.org/10.5194/gmd-7-1803-2014

Siegel LS, Homer J, Fiddaman T, McCauley S, Franck T, Sawin E, Jones AP, Sterman J, Interactive C.,2018. En-roads simulator reference guide. Technical Report.

Slangen, A.B.A., Adloff, F., Jevrejeva, S., Leclercq, P.W., Marzeion, B., Wada, Y., Winkelmann, R. 2017. A Review of Recent Updates of Sea-Level Projections at Global and Regional Scales. In: Cazenave, A., Champollion, N., Paul, F., Benveniste, J. (eds) Integrative Study of the Mean Sea Level and Its Components. Space Sciences Series of ISSI, vol 58. Springer, Cham. https://doi.org/10.1007/978-3-319-56490-6_17

Smith C J, Forster PM, Allen M, Leach N, Millar RJ, Passerello G A, Regayre LA. 2018. FAIR v1.3: a simple emissions-based impulse response and carbon cycle model. Geoscientific Model Development 11(6): 2273–2297. https://doi.org/10.5194/gmd-11-2273-2018

Smith C, Hall B, Dentener F, Ahn J, Collins W , Jones C , Meinshausen M, Dlugokencky E, Keeling R, Krummel P, Mühle J, Nicholls Z, Simpson I . 2021. IPCC Working Group 1 (WG1) Sixth Assessment Report (AR6) Annex III Extended Data (v1.0) [Data set]. Zenodo. https://doi.org/10.5281/zenodo.5705391

Smith CJ, Forster PM, Berger S, Collins W, Hall B, Lunt D, Palmer MD, Watanabe M, Cain M, Harris G, Leach NJ, Ringer M, Zelinka M. 2021. Figure and data generation for Chapter 7 of the IPCC's Sixth Assessment Report, Working Group 1 (plus assorted other contributions). Version 1.0. https://doi.org/10.5281/zenodo.5211357

Smith, C.J., Walsh, T.,, Borger, A., Forster, PGillett, N., Hauser, M., Lamb,W., Lamboll, R., Palmer, M., Ribes, A., Schumacher, D., Seneviratne, S., Trewin, B., and von Schuckmann, K., 2023. Indicators of Global Climate Change 2022 (v2023.06.02). Zenodo. https://doi.org/10.5281/zenodo.8000192

Smith CJ, Forster PM, Berger S, Collins W, Hall B, Lunt D, Palmer MD, Watanabe M, Cain M, Harris G, Leach NJ, Ringer M, Zelinka M. 2021. Figure and data generation for Chapter 7 of the IPCC's Sixth Assessment Report, Working Group 1 (plus assorted other contributions). Version 1.0. https://doi.org/10.5281/zenodo.5211357

Smith, C.J., Harris, G.R., Palmer, M.D., Bellouin, N., Collins, W., Myhre, G., Schulz, M., Golaz, J.C., Ringer, M., Storelvmo, T. and Forster, P.M., 2021. Energy budget constraints on the time history of aerosol forcing and climate sensitivity. Journal of Geophysical Research: Atmospheres, 126(13), p.e2020JD033622. https://doi.org/10.1029/2020JD033622

Smith, C., Hall, B., Dentener, F., Ahn, J., Collins, W., Jones, C., Meinshausen, M., Dlugokencky, E., Keeling, R., Krummel, P., Mühle, J., Nicholls, Z., & Simpson, I. (2021). IPCC Working Group 1 (WG1) Sixth Assessment Report (AR6) Annex III Extended Data (v1.0) [Data set]. Zenodo. https://doi.org/10.5281/zenodo.5705391

Sohag K, Chukavina K, Samargandi N. 2021. Renewable energy and total factor productivity in OECD member countries. Journal of Cleaner Production 296: p.126499. https://doi.org/10.1016/j.jclepro.2021.126499

Solaun, K. and Cerdá, E., 2019. Climate change impacts on renewable energy generation. A review of quantitative projections. Renewable and sustainable energy Reviews, 116, p.109415. https://doi.org/10.1016/j.rser.2019.109415

Statista - The Statistics Portal for Market Data, 2023, https://www.statista.com/

Statistical Review of World Energy, 2022. https://www.bp.com/en/global/corporate/energy-economics/statistical-review-of-world-energy.html

Steffen W, Richardson K, Rockström J, Schellnhuber HJ, Dube OP, Dutreuil S, Lenton TM, Lubchenco J. 2020. The emergence and evolution of Earth System Science. Nature Reviews Earth & Environment 1(1): 54-63.. https://doi.org/10.1038/s43017-019-0005-6

Sterman, J., 2000. Business Dynamics: Systems Thinking and Modeling for a Complex World Irwin McGraw-Hill Boston MA.

Sterman, JD, 1987. Systems simulation. Expectation formation in behavioral simulation models. Behavioral science, 32(3), pp.190-211. https://doi.org/10.1002/bs.3830320304

Supran, G., Rahmstorf, S. and Oreskes, N., 2023. Assessing ExxonMobil's global warming projections. Science, 379(6628), p.eabk0063. doi: 10.1126/science.abk006.

The Climate Action Tracker, 2023. https://climateactiontracker.org/

The Organisation for Economic Co-operation and Development (OECD), 2023, https://www.oecd.org/agriculture/topics/water-and-agriculture/

The World Bank 2022, World Bank Open Data, viewed December 2022. https://data.worldbank.org/

Thornton PE, Calvin K, Jones AD, Di Vittorio AV, Bond-Lamberty B, Chini L, Shi X, Mao J, Collins WD, Edmonds J, Thomson A. 2017. Biospheric feedback effects in a synchronously coupled model of human and Earth systems. Nature Climate Change 7(7): 496–500. https://doi.org/10.1038/nclimate3310

Tilman, D., Balzer, C., Hill, J. and Befort, B.L., 2011. Global food demand and the sustainable intensification of agriculture. Proceedings of the national academy of sciences, 108(50), pp.20260-20264. https://doi.org/10.1073/pnas.1116437108

Topuz SG. 2022. The Relationship Between Income Inequality and Economic Growth: Are Transmission Channels Effective? Social Indicators Research 162 (3): 1177–1231. https://doi.org/10.1007/s11205-022-02882-0

Tucker M., 1995. Carbon dioxide emissions and global GDP. Ecological Economics 15(3): 215-223. https://doi.org/10.1016/0921-8009(95)00045-3

Turnovsky SJ. 2015. Economic growth and inequality: The role of public investment. Journal of Economic Dynamics and Control 61: 204-221. https://doi.org/10.1016/j.jedc.2015.09.009

United Nations, Department of Economic and Social Affairs, Population Division (2022). World Population Prospects 2022, Online Edition https://population.un.org/wpp/Download/Standard/MostUsed/

United Nations, Department of Economic and Social Affairs, Population Division (2022). World Population Prospects 2022, Online Edition. https://population.un.org/wpp/Download/Standard/MostUsed/

Wakeland, W. and Homer, J., 2022. Addressing parameter uncertainty in a health policy simulation model using monte carlo sensitivity methods. Systems, 10(6), p.225. https://doi.org/10.3390/systems10060225

Walker R, Wakeland W. 2011. Calibration of complex system dynamics models: a practioner's report.

Walsh, B., Ciais, P., Janssens, I.A., Penuelas, J., Riahi, K., Rydzak, F., Van Vuuren, D.P. and Obersteiner, M., 2017. Pathways for balancing CO2 emissions and sinks. Nature communications, 8(1), p.14856. doi: 10.1038/ncomms14856 (2017)

West J, Bailey I, Winter M. 2010. Renewable energy policy and public perceptions of renewable energy: A cultural theory approach. Energy policy 38(10): 5739-5748. https://doi.org/10.1016/j.enpol.2010.05.024

Wigley, T. M. L., and S. C. B. Raper. 2005. Extended scenarios for glacier melt due to anthropogenic forcing, *Geophys. Res. Lett.*, 32, L05704, doi:10.1029/2004GL021238.

Wild, M., Folini, D., Henschel, F., Fischer, N. and Müller, B., 2015. Projections of long-term changes in solar radiation based on CMIP5 climate models and their influence on energy yields of photovoltaic systems. Solar Energy, 116, pp.12-24. https://doi.org/10.1016/j.solener.2015.03.039

Wilson, C., Guivarch, C., Kriegler, E., Van Ruijven, B., Van Vuuren, D. P., Krey, V., ... & Thompson, E. L. (2021). Evaluating process-based integrated assessment models of climate change mitigation. Climatic Change, 166, 1-22. https://doi.org/10.1007/s10584-021-03099-9

Wong, T. E., Bakker, A. M. R., Ruckert, K., Applegate, P., Slangen, A. B. A., and Keller, K. 2017. BRICK v0.2, a simple, accessible, and transparent model framework for climate and regional sea-level projections, Geosci. Model Dev., 10, 2741–2760, https://doi.org/10.5194/gmd-10-2741-2017

Woodard D L, Davis SJ, Randerson JT. 2019. Economic carbon cycle feedbacks may offset additional warming from natural feedbacks. Proceedings of the National Academy of Sciences 116(3): 759-764. https://doi.org/10.1073/pnas.18051871